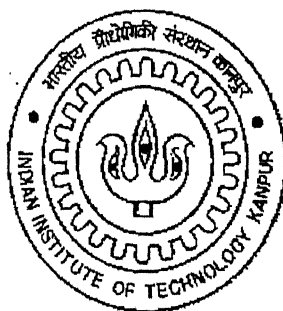


Studies on Micellar Enhanced Ultrafiltration for the Removal of Hexavalent Chromium

*A thesis submitted
in partial fulfillment of the requirements
for the degree of
Master of Technology*

**By
Gargi Ghosh**



to the
DEPARTMENT OF CHEMICAL ENGINEERING
INDIAN INSTITUTE OF TECHNOLOGY, KANPUR
JULY, 2002

5 FEB 2003 / CHE

पुरुषोत्तम कवचिन्धु के. कर पुस्तकालय

भारतीय प्रौद्योगिकी संस्थान कानपुर

अवधि क्र० A **141945**




A141945

CERTIFICATE



This is to certify that the thesis work entitled, "**Studies on Micellar Enhanced Ultrafiltration For The removal of Hexavalent Chromium**", by Gargi Ghosh has been carried out under my supervision and that it has not been submitted elsewhere for a Degree.

10th July, 2002


Dr. P.K. Bhattacharya

Professor

Department of Chemical Engineering

Indian Institute of Technology

Kanpur- 208016

Acknowledgements

To **Prof. P. K. Bhattacharya**, doing research under whose guidance is a seminal experience. He was there always by my side, during those long agonies and those sudden ecstasies. It is beyond my capacity to express the proper gratitude towards him. Words seem too feeble, too futile.

I would also like to thank **Dr. N. Verma** without whose help and co-operation the completion of this thesis would not have been possible.

A special thank goes to my friend **Debasish** who helped me throughout the modeling part of the work. I feel without his help this part of the thesis would have remained a daydream only. In this respect, I would like to thank few of my other friends, **Saurav**, **Partha**, **Arijit** and **Tirtha** who have always extended their helping hands whenever I was in sheer need.

My thank to all my lab-mates **Asit**, **Sujatha**, **Mr. Ramesh Chandra** and **Mr. Nagendra** for maintaining a healthy working atmosphere. I am also thankful to **Mr. S.V. Satyanarayana** for his kind co-operation during all the stages of my thesis work. A thank is due to my friends, **Prakash**, **Dulal**, **Jyoti**, **Aditi**, **Anisia** and **Monika** who have shared my joys and sorrows.

This acknowledgement will not be complete if I do not mention the impact of my stay in IIT, Kanpur. Leading a hostel life for the first time ever in my life, I had come to know so many different people with totally different outlooks towards the life and developed new friendships. However, most importantly I had come to understand the importance of sticking together through thick and thin and sharing feelings. Being away from the protected shelter of parents these experiences will surely help me to come out as a better human being. To be candid, I had enjoyed every bit of life in IIT and shall always cherish the memory of these days whenever I shall be going down the memory lanes.

And lastly but most importantly I convey my gratitude to all my **family members**. The greatest respect always shows itself in silence.

Gargi Ghosh

Abstract

Micellar Enhanced Ultrafiltration (MEUF) experiments were carried out using cetyl pyridinium chloride (CPC) as the surfactant wherein an attempt has been made to analyse the adsorption of chromate ions on the surfaces of the surfactant micelles. The influence of independent variables were studied on the permeate flux and retention of both, the surfactant as well as the chromate ions. It was observed that for a particular ^{pressure,} the flux was constant against constant bulk concentration of CPC and chromate ions, suggesting negligible concentration polarisation. There was distinct evidence of adsorption or distribution of metal ion between the aqueous surfactant monomer phase and micellar phase. The equilibrium adsorption coefficient (K_{ad}) for chromate ions were found out with the help of MEUF results. The value of K_{ad} was found to vary with the feed surfactant concentration.

It was observed that at high feed concentration even though the percent retention of chromate ion increased the flux declined, over a varying range of feed surfactant concentration. It was also found that at a higher surfactant concentration (60mM) the retention of chromate ion decreased. Further, the exclusive experimental runs with chromium ion solution gave an initial rapid decline of retention with pressure from 10 to 3%. This drop in retention was due to adsorption on polymeric membrane surface.

A mathematical model was developed to predict the permeate concentrations under varying operating conditions. The predicted flux and that obtained during the experiments were found to match closely. Predicted values could help in analyzing the MEUF system.

Nomenclature

a	molar extinction coefficient ($\text{mole}^{-1}\text{l}^{-1}$)
A	membrane area (m^2), absorbance
C	concentration (mole/l)
D	diffusivity (m^2/s)
f	activity coefficient
G	free energy (J/mole)
H	enthalpy (J/mole)
J	permeate flux (m/s)
K_{ads}	Freundlich adsorption equilibrium constant
L	cell path length
M	molecular weight (g/mole), micelles
N	aggregation number
P	pressure (kPa)
R	gas constant (J/mole-K), resistance (m), rejection
S	entropy (J/mole-K)
t	time(s)
T	absolute temperature (K)
V	volume (m^3)
z	distance from the membrane surface

Greek letters

Δ	difference
λ	wavelength (nm)
μ	viscosity (Pa-s)
ν	kinematic viscosity (m ² /s)
π	osmotic pressure (kPa)
ρ	density (kg/m ³)
ϕ	association factor

Subscripts

ads	adsorption
b	bulk
c	hexavalent chromium
eq	equilibrium
f	feed, fouling
j	component
m	membrane
ma	mass action
M	micellar phase
o	observed, initial
p	permeate
ps	phase separation
r	real
s	surfactant
w	water

Superscripts

B	blank (exclusive)
0	standard state

Abbreviations

Amp	ampere
CFC	critical feed concentration
CMC	critical micellar concentration
CPC	cetyl pyridinium chloride
CTABr	cetyl trimethyl ammonium bromide
conc.	concentration
Hz.	Hertz
MAL	micellar aggregation layer
MEUF	micellar enhanced ultrafiltration
SDS	sodium dodecyl sulphate
SED	semi equilibrium dialysis
soln.	solution

List of Figures

	Pages
Fig. 1.1 Schematic of Micellar Enhanced Ultrafiltration to remove dissolved metal ion	4
Fig. 2.1 Structure of Surfactant	17
Fig. 2.2 Probable structure of Cetyl Pyridinium Chloride	18
Fig. 4.1 Ultrafiltration Cell	33
Fig. 5.1 Variation of CPC [30 mM] permeate flux with time	36
Fig. 5.2 Permeate Flux and CPC Rejection vs. Applied Pressure	37
Fig. 5.3 Percent Rejection vs. Time plot of 30 mM CPC solution	38
Fig. 5.4 Percent Rejection vs. Time plot at 580 kPa	40
Fig. 5.5 Permeate Flux vs. Feed CPC conc. at 580 kPa	41
Fig. 5.6 Permeate Conc. vs. Feed Conc. at 580 kPa	42
Fig. 5.7 Percent Rejection vs Feed Conc. (mM) at 580 kPa	44
Fig. 5.8 Plot of Percent Rejection vs Feed Conc. (mM) at 580 kPa	45
Fig. 5.9 Percent Rejection vs. Time Plot for 50 ppm Chromate soln.	46
Fig. 5.10 Percent Retention vs. Time plot of 50 ppm Chromate soln.	47
Fig. 5.11 Percent Rejection & Permeate Flux of Chromate soln. (50 ppm) as a function of Applied Pressure	48
Fig. 5.12 Variation of permeate flux as a function of time with [CPC]=30 mM	50
Fig. 5.13 Permeate Flux as a function of chromate concentration	51
Fig. 5.14 Variation of Percent Rejection as a function of time at [CPC]=30 mM	52
Fig. 5.15 Variation of permeate flux with time at [Cr(VI)] = 0.3 mM	54
Fig. 5.16 Percent Chromate Retention and Permeate Flux as a result of surfactant concentration	55
Fig. 5.17 Variation of Percent Rejection with time at [Cr(VI)] = 0.3 mM	56
Fig. 5.18 A plot of Percent Rejection and Permeate Flux as a function of applied pressure	58
Fig. 5.19 Freundlich plot for the adsorption of Cr(VI) on the micelle surface	59
Fig. 5.20 Adsorbed Chromate vs. Surfactant Concentration	60
Fig. 5.21 Variation of Permeate Flux of CPC [30 mM] with time during MEUF	62
Fig. 5.22 Permeate Flux of CPC (30 mM) as a function of Applied Pressure (kPa)	63
Fig. 5.23 Variation of CPC (30 mM) permeate concentration with time	

during MEUF.	64
Fig.5.24 Variation of CPC permeate concentration with time during MEUF	65
Fig.5.25 Variation of Chromate (50 ppm) permeate concentration with time	66
Fig.5.26 Variation of chromate permeate concentration with time	67

List of Figures

	Pages
Fig. 1.1 Schematic of Micellar Enhanced Ultrafiltration to remove dissolved metal ion	4
Fig. 2.1 Structure of Surfactant	17
Fig. 2.2 Probable structure of Cetyl Pyridinium Chloride	18
Fig. 4.1 Ultrafiltration Cell	33
Fig. 5.1 Variation of CPC [30 mM] permeate flux with time	36
Fig. 5.2 Permeate Flux and CPC Rejection vs. Applied Pressure	37
Fig. 5.3 Percent Rejection vs. Time plot of 30 mM CPC solution	38
Fig. 5.4 Percent Rejection vs. Time plot at 580 kPa	40
Fig. 5.5 Permeate Flux vs. Feed CPC conc. at 580 kPa	41
Fig. 5.6 Permeate Conc. vs. Feed Conc. at 580 kPa	42
Fig. 5.7 Percent Rejection vs Feed Conc. (mM) at 580 kPa	44
Fig. 5.8 Plot of Percent Rejection vs Feed Conc. (mM) at 580 kPa	45
Fig. 5.9 Percent Rejection vs. Time Plot for 50 ppm Chromate soln.	46
Fig. 5.10 Percent Retention vs. Time plot of 50 ppm Chromate soln.	47
Fig. 5.11 Percent Rejection & Permeate Flux of Chromate soln. (50 ppm) as a function of Applied Pressure	48
Fig. 5.12 Variation of permeate flux as a function of time with [CPC]=30 mM	50
Fig. 5.13 Permeate Flux as a function of chromate concentration	51
Fig. 5.14 Variation of Percent Rejection as a function of time at [CPC]=30 mM	52
Fig. 5.15 Variation of permeate flux with time at [Cr(VI)] = 0.3 mM	54
Fig. 5.16 Percent Chromate Retention and Permeate Flux as a result of surfactant concentration	55
Fig. 5.17 Variation of Percent Rejection with time at [Cr(VI)] = 0.3 mM	56
Fig. 5.18 A plot of Percent Rejection and Permeate Flux as a function of applied pressure	58
Fig. 5.19 Freundlich plot for the adsorption of Cr(VI) on the micelle surface	59
Fig. 5.20 Adsorbed Chromate vs. Surfactant Concentration	60
Fig. 5.21 Variation of Permeate Flux of CPC [30 mM] with time during MEUF	62
Fig. 5.22 Permeate Flux of CPC (30 mM) as a function of Applied Pressure (kPa)	63
Fig. 5.23 Variation of CPC (30 mM) permeate concentration with time	

List of Tables

	Pages
Table A1. Water flux vs. Applied pressure	73
Table A2. Molar extinction coefficients	73
Table B1 Percent Rejection vs. time for CPC below CMC	75
Table B2 Permeate Flux and CPC Rejection vs. time at feed CPC = 30 mM	75
Table B3 Permeate Flux and Permeate Concentration of CPC in stirred and unstirred cell	76
Table B4 Permeate Flux and Permeate Concentration of Cr (VI) vs. time	76
Table B5 Permeate Flux vs. time at feed CPC = 30 mM	77
Table B6 Percent Rejection vs. time at feed CPC = 30 mM	77
Table B7 Permeate Flux vs. time at feed Chromate = 0.3 mM	78
Table B8 Percent Rejection vs. time at feed Chromate = 0.3 mM	78
Table B9 Permeate Flux vs. time	79
Table B10 Percent Rejection vs. time	79
Table B11 Permeate Flux and Percent Rejection vs. Pressure at [Cr (VI)] = 0.5mM	79
Table C1 Variation of K_{ad} with surfactant concentration	80
Table D1 Chromate conc. in permeate compartment vs. time	80
Table E1 Physical constants of surfactant	81

Contents

	Page
1. Introduction	1
2. Literature Review	
2.1 Separation Processes for the Removal of Metal Ions from Aqueous Streams	5
2.1.1 Other Separation Processes for the Removal of Chromium	6
2.2 Micellar Enhanced Ultrafiltration (MEUF)	8
2.2.1 Removal and Recovery of Organic Solutes	8
2.2.2 Separation and Concentration of Metal Ions	9
2.2.3 Miscellaneous Applications of MEUF	11
2.3 Structure of Surfactants	12
2.4 Micelles: Structures and Properties	14
2.5 Selection of Surfactant	15
2.6 Recovery of Surfactant	16
3. Theoretical Considerations	
3.1 Micelle	19
3.1.1 Aggregation Number	19
3.1.2 Concentration of Micelle	19
3.1.3 Thermodynamics of Micelle Formation	20
3.1.4 Mechanism of Micelle Formation	21
3.2 Ultrafiltration	21
3.2.1 Permeate Flux in UF	22
3.3.2 Real and Observed Rejection	23
3.3 Semi equilibrium Dialysis (SED)	23
3.4 Adsorption	24
3.5 Concentration measurement using UV-VIS spectrophotometer	24
3.6 Diffusivity Measurement	25
3.7 Development of Model	25
3.7.1 Species balance for the metal ions ($j = 1$)	26
3.7.2 Species balance for surfactant monomer ($j = 2$)	26

4. Experimental Work

4.1 Membrane and Chemicals	28
4.2 Instruments and other Auxiliaries	29
4.3 Solutions	29
4.4 Measurement of Density and Viscosity	29
4.5 Design of Experiments	29
4.6 Experimental Procedure	30
4.7 Measurement of Concentration	31

5. Results and Discussion

5.1 Selection of Operating Conditions	34
5.2 Micellisation and Ultrafiltration of Surfactant Solution	35
5.3 Ultrafiltration of Chromate in absence of Surfactant	42
5.4 Separation of Chromate using Surfactant Solution	49
5.5 Analysis of result through developed model	61

6. Conclusions and Recommendations

6.1 Conclusions	68
6.2 Recommendations	69

References 70**Appendix A** 73**Appendix B** 75**Appendix C** 80**Appendix D** 80**Appendix E** 81**Appendix F** 81

Chapter 1

Introduction

One of the most common problems confronted by chemical engineers today is the removal of heavy metals contaminated in wastewaters. Such effluent streams generate from industries like plating, tanneries, photographic, etc. Generally, most of the metal ions pollutants are non-biodegradable and quite a few of them are highly toxic and have carcinogenic effect. The traditional techniques, like the process of reduction or lime precipitation process, for the removal of metal ions from the aqueous effluents are not able to reduce the concentration to the levels required as per wastewater norms. The processes like activated carbon adsorption, electrolytic removal, and ion exchange are useful and common; however, they have their own limitations. Several attempts have been made to search for alternative methods for the removal of metal ions from aqueous streams. One such route to look for alternative method is through the use of membrane separation process. These processes have immense capabilities to treat wastewater containing toxic metal ions. Processes like reverse osmosis (RO), nanofiltration may be applied, using ion – selective membranes, considering the size of the ions in the solution. However, the permeate flux of RO membranes is limited [1] and requires high transmembrane pressure which makes the process expensive.

A new modified version of ultrafiltration (UF) process, called Micellar Enhanced Ultrafiltration (MEUF), is being developed. The process is proving effective in treating effluents.

MEUF has come into picture because of the extensive research carried out over the last decade to improve the performances of surfactant based separation processes. In this process, surfactant is added to the effluent stream at a concentration greater than the Critical Micellar Concentration (CMC) so that they form aggregates of about 50-150 molecules, called micelles [2]. If the tendency for the metal ion to be attracted on the micelle surface or for the organic molecules to be solubilised in the micelle interior is strong, a large fraction of the metal ions or dissolved organic molecules are trapped by micelles. When this solution is made to pass through an UF membrane, the

micelles along with the bound ions are retained. The permeate contains a very low concentration of the metallic ions or organic solutes (Fig.1.1). The process is versatile enough to include the separation of hydrocarbons, removal and recovery of organic acids and amines, apart from the separation and concentration of metal ions.

Theoretically, the metal ion concentration in the permeate should be equal to or less than the concentration of the unbound ions in the retentate. Similarly, the surfactant concentration in the permeate may be found equal to or less than the surfactant monomer concentration in the retentate. As either of these two concentrations are low, the permeate thus obtained may be of high purity. The retentate stream can then be treated for the recovery of the metallic ion and the surfactant.

In the design of MEUF process, the effect of operating parameters on the efficiency of the process, permeate flux and retention of micelles along with metal ions and quality of permeate concentrations are to be properly understood. Markels et.al [3] carried out MEUF in an unstirred batch cell and had proposed an unsteady state mass transfer model to describe the retention characteristics of the membrane. The model helps to estimate the intrinsic retention for both, the surfactant and organic solute and describes the physics at the membrane surfaces. Markels et.al [4] had also conducted crossflow ultrafiltration of micellar solutions. A steady state fouling resistance and osmotic pressure model was proposed by them to predict flux in crossflow MEUF process.

Suitability of surfactant is decided on the basis of the extent of solubilisation of organic solute or adsorption of metallic ions on the surface of the micelles. It has been observed that the surfactant having charge opposite to that of the target ions has higher efficiency in entrapping the solute or metal ions. The binding of hydrophobic solutes to both ionic and nonionic solutes were considered and was shown to be a function of the molecular structure of the surfactants, the concentration of the surfactant and the electrolytic composition of water [5].

Hexavalent chromium is known for toxicity as compared to trivalent ion. However, most of the industries like electroplating (electronic components electroplating) and leather industries, which are heavy users of chromium salts, generate in most cases aqueous effluents containing hexavalent chromium ions. Being highly toxic, its permissibility for the disposal of inland water by Indian Standard is 0.1 g/m^3 . Such a low concentration is difficult to achieve in processing industries for the disposal. Hence, it has become almost imperative for these industries generating hexavalent

chromium to look for attractive alternative methods, other than the conventional methods, for its disposal and/or use. The spent chrome liquor may be subjected to one of the fast emerging membrane separations technologies. One such separation technology, called electrodialysis (ED) selectively separates the neutral salts from chromium that may afford two streams. One containing neutral salts largely and the other chromium primarily. The reuse of two such streams can then easily be made. Further, there are evidences for the recovery of hexavalent chromium by MEUF, which have been studied [6]. These results are mostly to observe the influence of operating conditions. Rejection coefficients higher than 99% had been reported [7] at the varying conditions of pressure, feed surfactant concentration, etc.

The present work has been undertaken to study the adsorption of chromate ions on the micelle surface. Once the concentration of chromate present in the micelle phase is known, the equilibrium adsorption constant can be found out considering the adsorption isotherm to follow Freundlich adsorption isotherm. In this work, cetyl pyridinium chloride (CPC), a cationic surfactant was taken along with potassium chromate (anionic solute) in 0.01M Sodium Chloride (NaCl) medium.

With the above introduced background and importance of topic, the broad objectives for the present work may be drawn as follows:

- (1) To study the influences of operating conditions (concentration of surfactant, concentration of hexavalent chromium ion, pressure, and time) on permeate flux and the respective rejections/retentions.
- (2) To fundamentally study the permeate flux and rejection/retention patterns against operating conditions with exclusive experimental runs of CPC and chromium solution.
- (3) To observe the amount of adsorption of chromium on micelles against operating conditions.
- (4) To mathematically analyse the MEUF system and thereby develop a model to predict flux and permeate concentration.

Micellar Enhanced Ultrafiltration

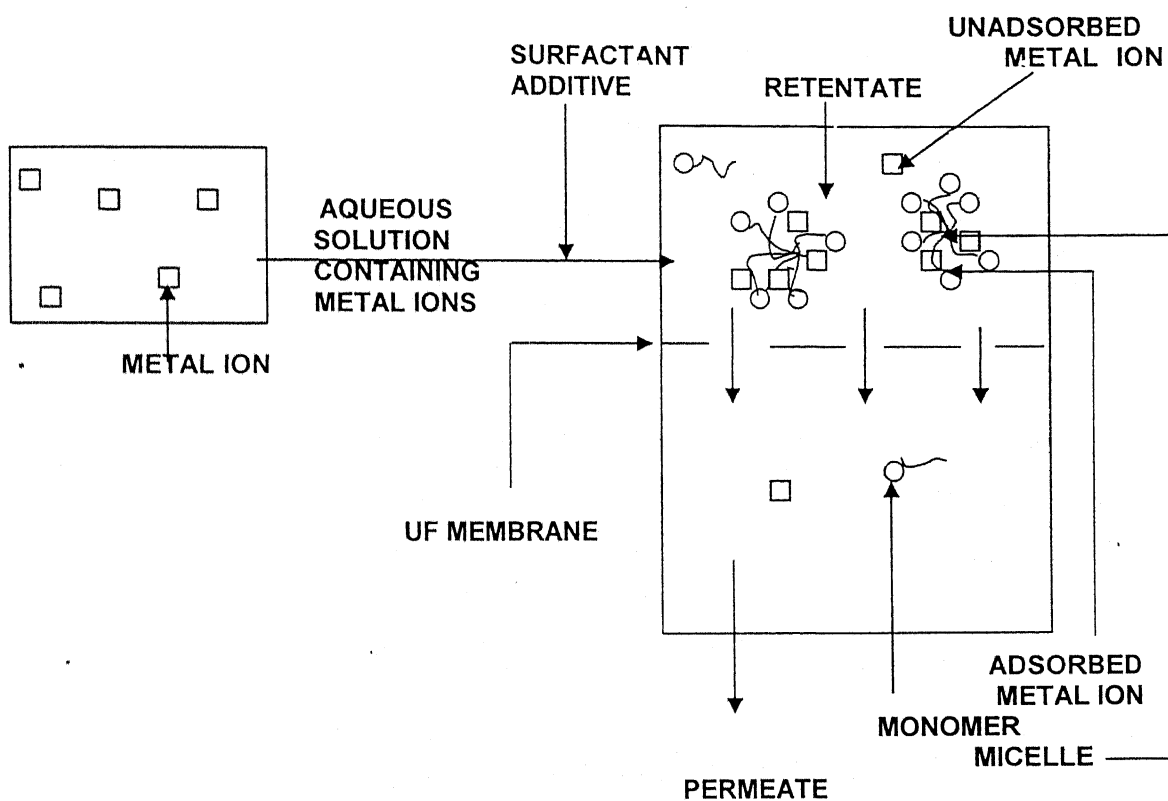


Fig. 1.1 Schematic of Micellar Enhanced Ultrafiltration to remove dissolved metal ions from water

Chapter 2

Literature Review

2.1 Separation Processes for the Removal of Metal Ions from Aqueous Stream

The removal of metal ions from aqueous streams is gaining importance as the environmental pollution control laws are becoming stringent. Some of the common processes employed for removal of these ions from wastewater streams are electrolytic method, ion exchange method, activated carbon adsorption, cellulose xanthate process, solvent extraction etc. However, the conventional treatment like hydroxide precipitation, electrolytic method, sulphide precipitation, has many inherent disadvantages. These are generation of sludge, loss of expensive chemicals to wastewater, cost of treatment chemicals. Among these sludge generation and disposal is the most pressing problem.

Ion Exchange Process

Ion exchange is a reversible chemical reaction wherein an ion from solution is exchanged for a similarly charged ion attached to an immobile solid particle. These solid ion exchange particles are either naturally occurring inorganic zeolites or synthetically produced organic resins. The synthetic organic resins are the predominant type used today because their characteristics can be tailored to specific applications.

Following is the selectivity sequence of an anion exchange resin:

citrate>sulphate>oxalate>iodide>nitrate>chromate>bromate>SCN>chloride>formate
>acetate>fluoride>hydroxide.

Even though ion exchange is suitable for treatment or materials recovery from very dilute solutions, the process is expensive as ion exchange resins and regenerating chemicals are costly.

Activated Carbon Adsorption

Activated Carbon Adsorption is an emerging technology for removal of inorganic species from wastewater such as cyanides, hexavalent chromium (Cr^{6+}) and cadmium. Adsorption is defined as the collection of a substance onto the surface of adsorbent solids. It is the removal process where certain particles are bound to an adsorbent

particle surface by either chemical or physical attraction. The activated carbon is an effective adsorbent material due to its large number of cavernous pores, which provide a large surface area. However, the maximum adsorption capacity of carbon is much pH sensitive and decreases rapidly with the change in pH.

Activated carbon is expensive and need to be regenerated. The regeneration and disposal of carbon containing Cr^{6+} is by itself a problem. Moreover, this process fails to produce an effluent with Cr^{6+} concentration at per with wastewater disposal norms, particularly in the presence of high concentration of Cr^{6+} in the feed.

2.1.1 Other Separation Processes for the Removal of Chromium

Chromium Removal by Modified PVP coated Silica Gel

A reactive polymer, long alkyl quarternized poly(4- vinyl pyridine) (PVP) was synthesized [8] and coated on the surface of silica gel to produce a granular sorbent to remove Cr^{6+} from water. The research demonstrated that the synthesized PVP – coated silica gel (referred to as coated gel) could successfully remove Cr^{6+} from solution [8]. The adsorption of Cr^{6+} was found to be strongly influenced by pH.

Chromium Removal from wastewater with Sulphur Dioxide

Generally, heavy metal wastes can be precipitated as insoluble sulphides or metal hydroxides. However, to precipitate the chromium, at first the reduction of chromium from soluble form to an insoluble form is required. Then SO_2 is added to water to form sulphurous acid. The sulphur in the acid formed is the reducing agent while the acid helps to reduce the pH (2.0-2.5).

Step I:



Under this condition, chromium sulphate is completely soluble. The second step involves raising of pH level to 8 and 8.5 with a base, such as caustic soda. Then trivalent chromium precipitates as insoluble chromium hydroxide.

Step II:



Although the technique is quite satisfactory in terms of purging chromium, this produces solid residue, containing toxic compounds. The final disposal of which is

generally by land filling with high cost as well as with the possibility of ground water contamination.

Biological Removal of Chromium from Industrial Wastewater

The removal of Chromium and other heavy metals, in low concentrations, from industrial wastewater was studied using different biosorption systems: a) bacterial biofilm supported by activated carbon, b) breweries residual yeast biomass and c) purified alginate.

Above citations are some of the conventional processes with their associated disadvantages. With rising costs and stricter environmental norms, newer processes are being explored for the removal of metal ions. This paved the way for the emergence of membrane based separation process as an alternative to traditional separation processes. Membrane technology appears promising owing to low capital cost, low space requirement, low labour costs, low energy requirements, and negligible sludge.

The membrane processes, which are significantly useful for the purpose, are described below with their importance:

An emerging application of Microfiltration (MF) is in the treatment of wastewater, particularly municipal sewage. When operated in conjunction with high-speed bioreactors, very low overall detention times with excellent removal of particulates including bacteria and viruses, is reported in pilot trials [9].

One of the important applications of electrodialysis [ED] in wastewater treatment systems is in processing rinse waters from electroplating industries. ED has successfully treated dump leach water containing heavy metals. The regeneration of chemical copper plating baths is studied in a pilot plant stage [10]. ED as compared to reverse osmosis (RO) can use more thermally and chemically stable membranes and hence the process can run at elevated temperature and in solution of high and low pH. However, the disadvantage associated with ED is that it can remove only the ionic components.

Municipal water supplies are frequently of inadequate quality for industrial and commercial processes. RO is now widely used to upgrade these water supplies. The most important single application is the electronics industry, where high quality rinse water is essential. RO can be used for pollution control. Some specific applications include treatment of electroplating rinse waters to recover metals, in which the treated water is suitable for reuse.

To summarise the applications of membrane processes like RO, UF, MF and ED, it may be observed that all these processes essentially remove solutes from micro to macro levels with the exception of ED where ionic solutes are separated. There is practically no information available which describe the applications of these processes towards separation of metals in ionic form. The application of ED particularly for hexavalent chromium separation also does not find any mention in the literature with regard to present author's knowledge. However, there are reports of the use of integrated membrane processes, which may tackle the problem of metal ion separation. One such emerging process is micellar-enhanced ultrafiltration.

2.2 Micellar Enhanced Ultrafiltration (MEUF)

Micellar Enhanced Ultrafiltration can be used to remove dissolved multivalent ions from water [11]. An appropriate concentration of surfactant of opposite charge to that of the ions is added to the aqueous stream, so that a large fraction of the surfactant exists in the micellar form. The target ions get bound or adsorbed on the micelles due to electrostatic attraction. When the resulting solution is passed through an ultrafilter having pore diameters smaller than micelle diameter, most of the surfactant and metal ions entrapped in micelles remain in the retentate solution. The permeate solution passing through the membrane is in many cases practically pure water [11]. This process can also be used for the separation of hydrocarbons and removal and recovery of organic acids, alcohols, and amines [11].

2.2.1 Removal and Recovery of Organic Solutes

MEUF results for the removal of 4 tert-butyl- phenol (TBP) using CPC as surfactant were reported for membranes with pore sizes ranging from 1000 to 50,000 MWCO [11]. The removal of n-alcohols and cresols by MEUF using CPC as the surfactant was also reported [12]. The effect of retentate CPC concentration on permeate flux and permeate CPC concentration was studied [2]. Experimental work on micellar ultrafiltration of CPC solution in batch cell at constant flux was also carried out [3].

Separation of phenol and 4- nitrophenol by means of hexadecyltrimethylammonium bromide (CTAB), sodium dodecyl sulphate(SDS), alkyl polyglucoside (APG) and oxyethylated methyl dodecanoate (OMD) from water and NaHCO_3 solution was reported [13]. The approach has been made to evaluate the resistance of secondary

layer and its change as a function of flux, time and the effect of pollutants and modifiers.

MEUF was applied to mixtures containing phenol or O-cresol and simultaneously, Zn^{2+} and / or Ni^{2+} , using an anionic surfactant [14]. The results demonstrated that removal of organic solute was not significantly affected by the presence of metal ions and vice - versa. This is because, the predominant mechanism of removal of metal ions were totally different. The ability of MEUF to simultaneously remove organic and multivalent metal ionic solutes makes it economically attractive.

The effect of important operating parameters (applied pressure, concentration of solutes and surfactants) on the extent of separation of organic solutes (aniline and phenol) was observed [15]. Solubilisation of these solutes in CPC micelles was experimentally ascertained. Solubilisation equilibrium constant of phenols in CPC was estimated to be around four times that of aniline. A mathematical model developed in this study [16] was used to describe the separation of organic solutes by MEUF and predict permeate solute concentration under varying operating conditions. Equilibrium distribution constants of phenol between surfactant micelles and water were determined by MEUF using commercial ultrafiltering centrifuge tubes [17]. Three surfactants: sodium dodecyl sulphate (SDS), polyethylene 20 cetyl ether (C16E20) and cetylpyridium chloride (CPC) were tested with a 10,000 MWCO membrane.

A steady state combined resistance in series and osmotic pressure model was proposed [4] to predict the flux in laminar, cross flow ultrafiltration of micellar CPC solution. The data were obtained for CPC monomer – micellar equilibrium in aqueous solutions using UF [18].

2.2.2 Separation and Concentration of Metal Ions

The application of MEUF for removing heavy metal ions from water is getting noticed [18]. MEUF was found to be extremely effective in separating Cu^{2+} and a rejection of 99.8% was observed when present in dilute concentration [19]. However, the permeate purity decreased as the metal concentration in the feed increased. Further, purity also gets affected by the reduction in surfactant concentration and or with the presence of monovalent salt in the solution.

MEUF of gold (III) from hydrochloric acid media was also studied [20] using polyoxyethylene nonylphenyl ethers (PONPES) as a nonionic surfactant. The

rejection efficiency of gold (III) increased with increasing surfactant concentration, ethylene oxide number of PONPE and the applied pressure as well as decreasing molecular weight cut-off of the membrane. It was found that the use of MEUF with PONPE provides higher selectivity to gold (III) than those with charged surfactant such as cetyl pyridinium chloride (CPC) and sodium dodecyl sulphate (SDS).

Traces of aluminium were preconcentrated [21] in water by forming a complex with lumogallion. Thereafter, it was successfully accumulated in the micellar phase, obtained from cationic and non-ionic surfactants, and filtered through 10,000 MWCO ultrafiltration membranes. It was reported [21] that at pH 5.9, with 1×10^{-3} M lumogallion and 2×10^{-2} M cetyltrimethylammonium bromide, quantitative retention of aluminium present at $\mu\text{g/ml}$ concentration level was achieved.

Lecithin, a natural, nontoxic, and biodegradable surfactant exhibits emulsifying characteristics, which may be used for MEUF. The binding of various lecithin to cadmium, copper, lead, nickel and zinc in a mixture as well as individually were observed [22]. In the presence of all five heavy metals, the lecithin showed the higher affinity for Cu than for Cd and Zn whereas Ni was found to have the lowest affinity. The affinity for Cd and Zn were found to be similar. In experiment when only one metal was present, lecithin exhibited the following affinity: $\text{Ni} > \text{Cu}$ and $\text{Zn} > \text{Cd}$; whereas Cu and Zn show similar affinity. Lead was not bound significantly in the either scenario.

Industrial wastewater from metal plating, petroleum refining, chemical and food processing plants vary in composition and may contain toxic substances like heavy metal cations and chemical compounds in the aqueous phase and oil fractions. It had been proposed [23] to combine MEUF and algae containing membrane bioreactors (MB) to completely remove the metal ions from metal finishing industry's effluent. MEUF, with lecithin as surfactant, was found to remove heavy metals from aqueous (50 – 90% removal) and non aqueous wastes (90 -97% removal). Continuous binding and separation of the ions through membrane bioreactors that were 20 -50 times more efficient than conventional bioreactors, increased the efficiency of removal of trace levels of heavy metals.

The removal of hexavalent chromium by micellar enhanced ultrafiltration using cetyl trimethylammonium bromide (CTABr) as well as cetyl pyridinium chloride (CPC) were experienced [6,7]. Effect of metal ion concentration, surfactant concentration,

presence of monovalent salt against varied transmembrane pressure drop, feed velocity and temperature were studied. Rejection coefficients, higher than 99%, were obtained as long as the feed concentration is less than or equal to 200 times the standard. The rejection rate was found to depend on ionic strength and pH. The increase of ionic strength decreased the retention of chromate ions and permeate surfactant concentration. As long as the NaCl feed concentration was less than or equal to 100mM, more than 88% of hexavalent chromium were retained and surfactant leakage was reduced [6,7].

Addition of small concentration of nonionic surfactant to anionic surfactant results in anionic nonionic mixed micelles and exhibit negative deviation from ideality of mixing. This leads to smaller fraction of surfactant being present as monomer and subsequently a large fraction present in micellar form [24]. It was reported that addition of nonionic surfactant improved the separation of Zn^{2+} substantially at total concentration above CMC of anionic surfactant. Both Zn^{2+} and tert – butylphenol showed unexpected rejection at surfactant concentrations moderately below the CMC. This was considered to be due to a higher surfactant in the gel layer, adjacent to the membrane where micelles were present.

A lab study was conducted to evaluate the effects of composition and concentration of mixed anionic / nonionic surfactants on the study of MEUF operation for the removal of metal ions / organic solutes from aqueous solution [25]. Based on the analysis of surface tensions and micelle sizes, it was found that for mixed sodium dodecyl sulphate (SDS) / Triton X-100 surfactants, the CMC was significantly lower than that of SDS and formed mixed micelles. The rejection of Cu^{2+} was found to be negligible with a surfactant concentration 10mM, on using pure Triton X-100. Whereas the rejection increased upto 85% on increasing the SDS mole fraction, indicating the mechanism of Cu^{2+} rejection being chiefly due to the electrostatic attraction [24]. When MEUF technique was applied to Cu^{2+} and phenol simultaneously from aqueous solution, Cu^{2+} rejection was slightly enhanced in the presence of phenol [25]. However, rejection of phenol was comparatively low approx. 27%.

2.2.3 Miscellaneous Applications of MEUF

Micellar Enhanced Ultrafiltration was used to recover thuringiensin from the supernatant of *Bacillus thuringiensis* fermentation broth using CPC [26]. On manipulating various possible process variables, it was found that CPC concentration

and membrane pore size were the two major factors to the increase recovery of thuringiensin. It was also reported that ionic strength, pH adjustments were not necessary and micelle formation temperature was not important within the temperature range studied. The bioassay results showed that the spray-dried thuringiensin with CPC was more toxic to fly larvae than without CPC. This indicates that CPC not only facilitated thuringiensin recovery but also improved the insecticidal effect.

In ligand modified MEUF (LM-MEUF), a surfactant and ligand are added to an aqueous solution containing ions of like charge. The ligand forms complex with the target ions and becomes incorporated in the micelles. An economic analysis of LM-MEUF for 1×10^5 gal/day unit is reported [27]. The effect of important parameters including feed surfactant, ligand and copper concentration were studied. The result from the sensitivity analysis was used to compare the cost of removal and recovery of copper between the processes of LM-MEUF and solvent extraction process. The comparative economic analysis indicated a 17% higher capital and 43% higher operating cost for LM-MEUF process compared to solvent extraction process [26].

2.3 Structure of Surfactants

Surfactant is a diminutive term for SURFace ACTive AgeNT. Surfactants are materials that tend to not only accumulate at the surfaces or aggregate in solutions, but by their presence, they also change the properties of surfaces and solutions. More generally, they are active at the interfaces. Surfactant molecules have two distinct parts as shown in Fig. 2.1: one that has an affinity to the solvent (hydrophilic in case of aqueous solution) and the other that does not have any affinity (hydrophobic). It is the tendency of the hydrophobic part of the molecule to aggregate because of their mutual dislike for solvent. This dislike tends to become the driving force for the surfactant self – association. The hydrophilic head groups remain spaced out in the solution.

The properties of surfactants fall into two broad categories: adsorption and self – assembly.

Adsorption is the tendency for a surfactant molecule to collect at the interface. This molecular property leads to the macroscopic properties of wetting, foaming, and emulsion formation.

Self – assembly is the tendency for the surfactant molecules to organize themselves into extended structures in water. This includes the formation of micelles, bilayers and liquid crystals.

Surfactant can be broadly classified into ionic, nonionic and zwitter ionic classes.

Ionic can be both anionic and cationic surfactants [28].

Anionic Surfactant

This type of surfactant on dissociation in a liquid form results in a negatively charged ion. Commonly used anionic surfactants are alkyl sulfates, alkyl benzenesulfonates, alkyl sulfonates and the alkyl phosphates. In fact, probably the most studied surfactant over the years is one of the alkyl sulphates: sodium dodecyl sulphate.

Anionic surfactants are widely used .They are used in shampoos, in dishwashing detergents and in washing powders. In many industrial and commercial applications, they are used in conjunction with nonionic surfactants to provide even greater stability.

Cationic Surfactant

This type of surfactant on dissociation in a liquid form results in positively charged ion. Alkyl pyridinium and quarternary ammonium salts provide excellent surfactants that can be used over a range of conditions. Cetyl pyridinium chloride and cetyl trimethyl ammonium bromide are the most commonly used cationic surfactants. They are used in things like hair conditioner and fabric softeners. The fatty amine salts are quite useful along with nonionic surfactants, giving good stability over a range of pH levels.

Zwitter ionic or Amphoteric Surfactant

This type of surfactant contain both positive (cationic) and negative (anionic) groups. In acidic solutions they form cations and in alkaline solutions they form anions. Whereas, in the middle range of pH they become molecules with two ionic groups of opposite charges known as Zwitter ions. The key property of amphoteric surfactants is the compatibility with aqueous ions and being resistant to both acids and alkalis. Therefore, they are often used for foaming, wetting and emulsification in personal care products.

Non-ionic Surfactant

This type of surfactant on dissociation in liquid form does not result in either positively charged or negatively charged ions. They are referred chiefly to polyoxyethylene or polyoxypropylene derivatives. However, other surfactants are also

included such as, fatty alkanoamides and amine oxides. They are usually prepared by addition of ethylene oxide to alkyl phenols, fatty acids and alcohols, fatty mercaptans and amines [29].

Another class of nonionic surfactants is alkyl polyglycosides. At least, for the last 20 years, these have been dubbed the “new generation nonionic surfactants”. In these molecules, the hydrophilic group is sugar. Alkyl glycoside and glucose ester are examples of alkyl polyglycosides.

Nonionic surfactants differ from both cationic and anionic surfactants in that the molecules are actually uncharged. The hydrophilic group is made up of some other very water-soluble moiety, (e.g. a short, water-soluble polymer chain) rather than a charged species. Traditionally, nonionic surfactants have used polyethylene oxide chains as the hydrophilic group.

The predominant use of these surfactants is in food and beverages.

Nonionics do not contain ions and hence solubilise over the pH range. Their solubility is due to hydrogen bonding between the hydrophile and water molecules. Amphoterics have both anionic and cationic groups, so they are soluble in water over wide pH limits; even wider than nonionics. Whereas, nonionics lose their solubility at low and high pH, and at high electrolyte levels, as electrolytes competes with ethoxylate chain for hydrogen bonded water [30].

pH	1	2	3	4	5	6	7	8	9	10	11	12	13	14
Anionic														
Nonionic														
Cationic (weak)														
Cationic (quat)														
Amphoteric														

2.4 Micelles : Structures and Properties

When surfactant molecules are present in aqueous solution at concentrations above their critical micellar concentration (CMC), interactions between the hydrophobic alkyl chains of adjacent molecules provide a force tending to pack them closer to each other. The hydrophilic head groups, on the other hand, have a strong affinity for water and tend to remain spaced out in the aqueous medium. When the head groups are charged, electrostatic repulsion provides additional force tending to distance the head groups. These opposite forces govern the formation and growth of micelles. The

micelles continue to grow until the energy released from the condensation of alkyl chains is balanced by the work done to bring the hydrophilic head groups (which may be charged) into the micellar surface.

The existence of different shapes and sizes of micelles are described [11]. They are also interchangeable from one form to another. These are spherical, cylindrical, flexible- bilayer, planer- bilayer and inverted micelles, depending upon the conditions prevailing in the system. Micelles are not fixed entities but have a transient character. Surfactant molecules rapidly join and leave the molecules, whose aggregation number presents only an average over time. nice

Stigter [27] introduced a detailed model for ionic micelles. According to this model, the small micelle consists of a spherical hydrocarbon core and an aqueous *Stern layer*. The radius of the micelle is equal to the length of the alkyl tail of the surfactant. The *Stern layer* consists of hydrophilic heads of the surfactant molecules along with a fraction of the counter ions. Outside of the shear surface is the Gouy – Chapman diffuse double layer, which contains an excess of counter ions equal to the charge of the micelle. The model as applied to CPC is shown in Fig. 2.2.

2.5 Selection of Surfactant

In the selection of surfactant for use in MEUF, some important desirable characteristics are [11]:

- [1] high solubilisation capacity for the organic pollutant or adsorption capacity for metal ions
- [2] forms large micelles, so that large pore sizes can be used and
- [3] low monomer concentration, so that little surfactant is wasted

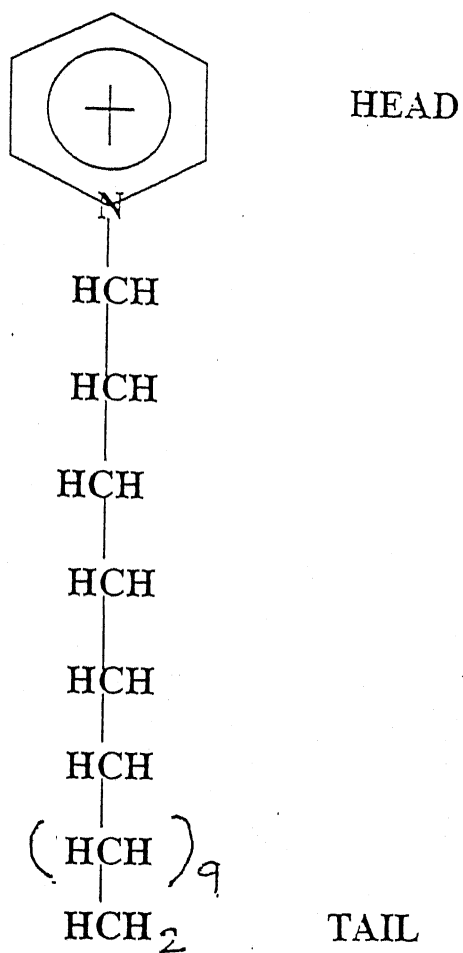
One desirable characteristic of a surfactant is a long hydrocarbon chain, since this result in the formation of larger micelles, high solubilisations and low monomer concentrations. Nonionic surfactants form large micelles and have low monomer concentrations in micellar solutions. However, the solubilisation or adsorption capacities of the nonionic surfactants are not high compared to anionic or cationic surfactants. Cationic surfactants generally have much lower Krafft temperature than those of anionic surfactants of corresponding hydrophobic group size. Therefore, cationic surfactants with large hydrophobic groups, resulting in large micelles, high solubilisation / adsorption capacities, and low monomer concentrations, may be used

in MEUF. Cationic surfactants do not pose significant environmental risks. In general, cationic surfactants are the surfactants of choice in MEUF.

2.6 Recovery of Surfactant

It is important to recover surfactant for reuse in order for the process to be economical. The recovered surfactant will normally be recycled to the process to minimize makeup surfactant requirements.

The process use precipitation of surfactant by using monovalent or multivalent counterions. The surfactant is precipitated from the aqueous solution by addition of an ion of opposite charge to that of the surfactant (the counterion). The precipitate is removed from solution by gravity settling, filtering, or centrifuging. This filter cake is then recycled or further treated if the counterion used for the precipitation is unacceptable in the process. Ultimate recoveries of 95% were shown to be attainable using this process [11].



CETYL PYRIDINIUM CHLORIDE
(CPC)

Fig. 2.1 Structure of the CPC monomer.

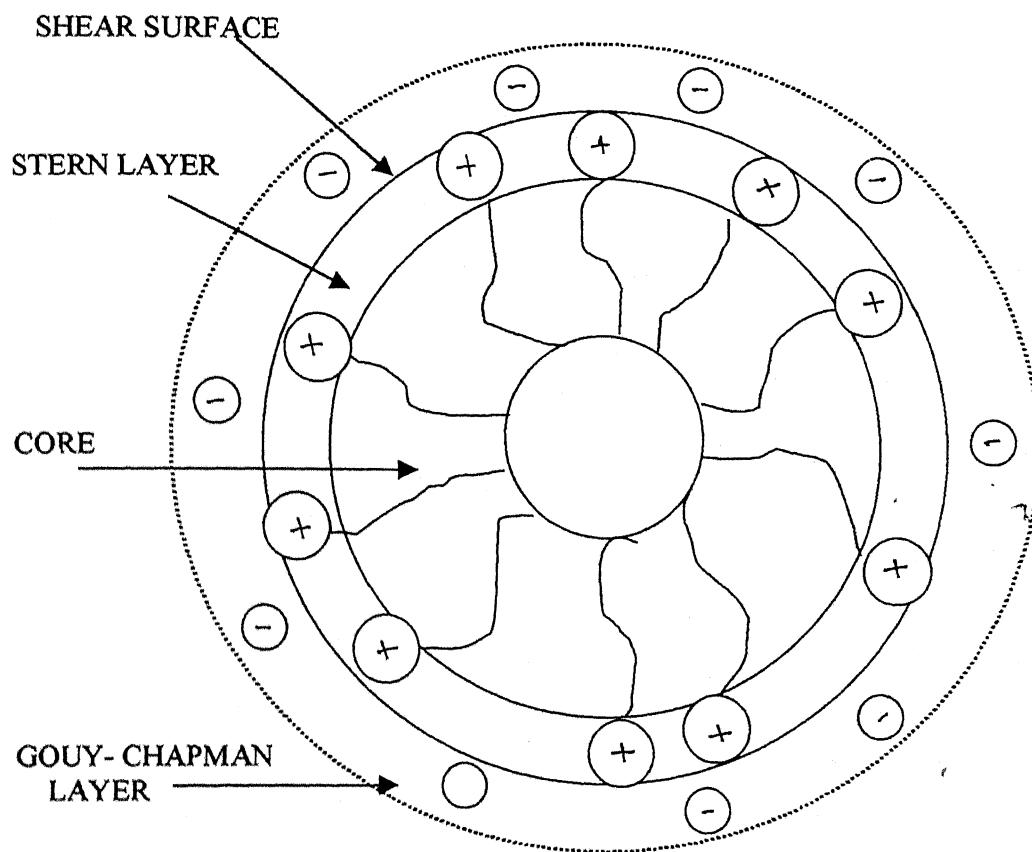


Fig.2.2 Probable structure of cetyl pyridinium chloride micelle

3.1 Micelle

When surfactants are added to aqueous streams above CMC, they form aggregates of about 50-150 molecules, called micelles. Micelles exist in different shapes and sizes. They are interchangeable from one form to another. Micelles are not fixed entities, but are dynamic in nature. The surfactant molecules rapidly join and leave the micelles, whose aggregation number is only an average over the time.

As described earlier micelle consists of a spherical hydrocarbon core and aqueous Stern layer. A probable structure of micelle is given in the Fig. 2.2. The radius of micelle is equal to the length of the alkyl tail of the surfactant.

3.1.1 Aggregation Number

The number of monomeric surfactant molecules contained in a micelle gives aggregation number. It can be obtained by dividing micellar molecular weight by monomeric molecular weight. Molecular weight of the micelles can be obtained from various techniques including gel filtration, light scattering, sedimentation equilibrium, and small angle X-ray scattering. Aggregation number is influenced by the ionic strength.

$$\frac{\text{micellar molecular weight}}{\text{monomeric molecular weight}} = \text{Aggregation number} \quad (3.1)$$

3.1.2 Concentration of Micelle

CMC may be defined as the lowest concentration above which the monomers cluster together to form micelles. Given CMC, concentration of surfactant and the aggregation number it is possible to calculate the concentration of micelles in moles/liter using the following equation:

$$[\text{micelles}] = \left(\frac{C_0 - \text{CMC}}{N} \right) \quad (3.2)$$

where N is the aggregation number.

3.1.3 Thermodynamics of Micelle Formation

Two general approaches deal with the micellization. In the first, micellization is regarded as a phase separation, which commences at CMC. CMC is taken to represent the saturation concentration for unaggregated surfactant. In the second approach, micelles and single surfactant ions are considered to be in association – dissociation equilibrium. The CMC in this approach is merely a concentration range above which most of the surfactant appears in micellar form.

Phase Separation Approach

The equilibrium between surfactant ions D^+ , counterions X^- and micelles M is as follows:



The micelle charged aggregate of surfactant ions plus an equivalent of counterions in the surrounding region are treated as a separate phase. The standard free energy of micellization per mole of monomer is given by [28]:

$$\Delta G_{ps}^0 = \frac{-RT}{j} \ln \left(\frac{f_M [M]}{f_D^j f_X^j [D^+]^j [X^-]^j} \right) \quad (3.4)$$

where $[M]$, $[D^+]$ and $[X^-]$ are equilibrium concentrations and f_M , f_D and f_X are the respective activity coefficients.

The standard heat of micellization is [28]:

$$\Delta H_{ps}^0 = -RT^2 \frac{d}{dT} \left[\ln (f_D f_X [CMC] [X^-]) \right] \quad (3.5)$$

The standard ^{entropy} ~~enthalpy~~ of micellization is given by [28]

$$\Delta S_{ps}^0 = \frac{(\Delta H_{ps}^0 - \Delta G_{ps}^0)}{T} \quad (3.6)$$

Mass Action Model

The equilibrium considered here is as follows:



where M^{+z} is thought to be an aggregate of j surfactant ions and $(j-z)$ firmly bound anions. The standard free energy of micellization per mole of monomeric surfactant ions is:

$$\Delta G_{ma}^0 = \frac{-RT}{j} \ln \left(\frac{f_M [M^{+z}]}{f_D^j f_X^{j-z} [D^+]^j [X^-]^{j-z}} \right) \quad (3.8)$$

When j is large, concentrations near [CMC] are used and when there is no added salt, then the above equation changes to:

$$\Delta G_{ma}^0 = \left(2 - \frac{z}{j} \right) RT \ln [CMC] \quad (3.9)$$

if z is zero i.e. j counterions are firmly bound to the micelle so as to give zero charge, the above equations reduces to

$$\Delta G_{ma}^0 = 2RT \ln [CMC] \quad (3.10)$$

If $z = j$, i.e. no counterions are bound to the micelles then equation (3.14) becomes

$$\Delta G_{ma}^0 = RT \ln [CMC] \quad (3.11)$$

The standard heat of micellization is given by

$$\Delta H_{ma}^0 = - \left(2 - \frac{z}{j} \right) RT^2 \frac{d \ln [CMC]}{dT} \quad (3.12)$$

3.1.4 Mechanism of Micelle Formation

The standard free energy of micellization is known to decrease with the increase in chain length [31]. This indicates that with increasing chain length, there is an increase in hydrophobicity of the surfactant. Therefore, the tendency for micelle formation also increases. Further, the tendency of micelle formation is also confirmed by a high positive value of standard entropy of micellization. The explanation for positive entropy values is as follows: alkyl chains induce a structured arrangement of water molecules around themselves. When micellization starts, the alkyl chains aggregate and the structured water molecules revert to ordinary bulk conditions with a considerable increase in entropy.

3.2 Ultrafiltration

Ultrafiltration refers to the separation from the solvent of solute molecules which are at least 10 times bigger than solvent molecules and can be as large as 0.5μ . As the smaller solutes permeate through the membrane, the larger ones are retained. This leads to an accumulation of retained components in the boundary layer adjacent the membrane surface. This phenomenon is referred to as Concentration Polarization. Under certain conditions as the concentration of rejected solute increases, large

molecular weight solutes may form a 'gel' which precipitates at the membrane surface. Such a precipitate may be in the nature of a cake or slimy deposit. It has the undesirable consequence of being a second membrane on top of actual UF membrane. The resistance to solvent flow through this cake can be substantial so that the solvent flux is reduced.

3.2.1 Permeate Flux in UF

The permeate flux through the porous membrane can be described by *Darcy's* law for flow through porous media. It states that the volumetric flux is directly proportional to the applied pressure gradient.

$$J = \frac{1}{A} \left(\frac{dV}{dt} \right) = \frac{\Delta P}{\mu_m R_m} \quad (3.13)$$

where R_m is the intrinsic hydraulic resistance of the membrane. It is a function of pore size, tortuosity, membrane thickness, and porosity. R_m is also a function of pressure history.

At low pressure, low feed concentrations and high feed velocity, i.e. under conditions where concentration polarization effects are minimal, the transmembrane pressure will affect flux. However, during UF of macromolecular solutes or at high pressure, the linear relationship between J and ΔP does not hold good because of concentration polarization [32].

From the concentration polarization model, it is evident that the concentration of the solute at the membrane surface is considerably higher than that in the bulk. The solute concentration on side of the membrane being high and on the other side being very low creates an osmotic pressure difference ($\Delta\pi$). This acts in opposition to applied pressure. So in equation 3.1 (ΔP) gets replaced by ($\Delta P - \Delta\pi$).

$$J = \frac{\Delta P - \Delta\pi}{\mu_m R_m} \quad (3.14)$$

In some situations, macromolecular solutes may get adsorbed and can foul the membrane and as well can form polarized layer. These phenomenon are incorporated in the above equation by introducing the resistance due to adsorption (R_a) and (R_p) that due to the formation of polarized layer. Therefore, the equation becomes:

$$J = \frac{\Delta P - \Delta\pi}{\mu_m (R_m + R_a + R_p)} \quad (3.15)$$

The osmotic pressure for CPC in 0.01M NaCl solutions was found experimentally by

[4]. The data curve was fitted and given by:

$$\pi = 0.00366C + 0.01209C^2 - 8.0 \times 10^{-5} C^3 + 2.592 \times 10^{-7} C^4 \quad (3.16)$$

for $C \leq 250 \text{ Kg/m}^3$ where π is in kPa and C is the total surfactant concentration in Kg/m^3 .

The following correlation was obtained for dependence of kinematic viscosity of CPC solutions on concentrations [16].

$$\nu_s = 9.98 \times 10^{-7} + 5.59 \times 10^{-9} C + 2.50 \times 10^{-11} C^2 - 1.43 \times 10^{-13} C^3 + 4.46 \times 10^{-16} C^4 \quad (3.17)$$

where C is in mM and ν_s is in m^2/s .

3.2.2 Real and Observed Rejection

In the membrane separation, the membrane rejection for a given solute is usually characterized by the intrinsic or real rejection coefficient. This is defined as

$$R_r = 1 - \frac{C_p}{C_m} \quad (3.18)$$

where C_p is the solute concentration in the permeate and C_m is the solute concentration at the membrane surface (retentate side). Since it is difficult to measure C_m experimentally, it is replaced by the bulk retentate concentration C_b , which can be easily measured.

The observed rejection coefficient is defined by the following equation:

$$R_o = 1 - \frac{C_p}{C_b} \quad (3.19)$$

However, the observed rejection coefficient is not a property of the membrane but depends strongly on experimental conditions under which it is determined.

3.3 Semi equilibrium Dialysis (SED)

In SED experiments, concentrations of low molecular weight solutes are determined on both sides of the dialysis membrane, after sufficient time has elapsed so that equilibrium is reached with respect to these solutes. However, equilibrium is not reached by the surfactant, which continues to have a much greater concentration and a slightly greater thermodynamic activity in the retentate solution than in the permeate. The method is called "semiequilibrium" dialysis as only the solutes (not the surfactant) reaches equilibrium with respect to both the retentate and permeate solution. The surfactant continues to diffuse through the membrane for long periods

of time, although within a 24-hr period its concentration in the permeate compartment usually does not exceed the CMC.

3.4 Adsorption

When surfactant is added to an aqueous solution containing the target ions at a concentration greater than CMC, the counter ions get adsorbed onto the surface of the micelles formed. Adsorption isotherm is the equilibrium relationship between adsorbed concentration (C_{ads}) and dissolved equilibrium concentration (C_{eq}). The *Freundlich* equation is expressed as:

$$C_{ads} = K_{ad} C_{eq}^{1/n} \quad (3.20)$$

Equation 3.20 can be linearised as follows:

$$\log C_{ads} = \log K_{ad} + 1/n \log C_{eq} \quad (3.21)$$

where $1/n$ is *Freundlich* constant ($\mu g/g$) and K_{ad} is the *Freundlich* equilibrium constant.

When $n = 1$, *Freundlich* gives rise to linear isotherm.

On the micelle phase boundary (neglecting the *Stern* layer thickness), the metal ion concentration is in equilibrium with the unadsorbed free ion concentration in the bulk phase [33].

3.5 Concentration measurement using UV- VIS spectrophotometer

According to Bouguer – Lambert – Beer (BLB) law, the absorbance at a particular wavelength for a single species is given by

$$A_{\lambda} = a_{\lambda} LC \quad (3.22)$$

where L is the cell path in cm, C is the concentration of the solute in mol l^{-1} and a_{λ} is the molar adsorption coefficient at wavelength λ in $\text{mol}^{-1}\text{cm}^{-1}$. The BLB law is usually valid for dilute solutions, for strongly monochromatic radiation and in optically homogeneous media. It is also valid for a mixture of absorbing species, if there are no mutual interactions, which would contravene the principle of additivity of absorbances.

Let A_1, A_2, \dots, A_n be the absorbances at wavelengths $\lambda_1, \lambda_2, \dots, \lambda_n$ for a sample containing n species. Then for $L = 1$ cm,

$$A_1 = a_{11}C_1 + a_{21}C_2 + \dots + a_{n1}C_n \quad \text{at } \lambda_1$$

$$A_2 = a_{12}C_1 + a_{22}C_2 + \dots + a_{n2}C_n \quad \text{at } \lambda_2$$

(3.23)

$$A_1 = a_{11}C_1 + a_{21}C_2 + \dots + a_{n1}C_n \quad \text{at } \lambda_1$$

$a_{11}, a_{21}, \dots, a_{n1}$ may be obtained from the pure component absorbances for the n species at wavelengths $\lambda_1, \lambda_2, \dots, \lambda_n$. A_1, A_2, \dots, A_n are measured using a spectrophotometer. The equations (3.23) can be solved simultaneously to obtain the concentrations C_1, C_2, \dots, C_n of the n species.

3.6 Diffusivity Measurement

Diffusivity of chromate solution was found out using Wilke - Chang correlation. The equation is given below:

$$D_{AB} = \frac{7.4 \times 10^{-8} \times (\phi M_B)^{1/2} T}{\eta_B V_A^{0.6}} \quad (3.24)$$

where M_B is the molecular weight of the solvent, T is the temperature in K, η is viscosity, V_A is solute molal volume and ϕ is the association factor.

3.7 Development of Model

In an unstirred batch cell, the general solute mass balance equation can be derived as follows:

From Fick's second law, we get

$$\frac{\partial C_j}{\partial t} = D_j \left(\frac{\partial^2 C_j}{\partial x^2} + \frac{\partial^2 C_j}{\partial y^2} + \frac{\partial^2 C_j}{\partial z^2} \right) \quad (3.25)$$

Neglecting transfer in x and y direction, we get

$$\frac{\partial C_j}{\partial t} = D_j \left(\frac{\partial^2 C_j}{\partial z^2} \right) \quad (3.26)$$

Taking into account, the convective and diffusive flux of the solutes into the aggregation layer, the general solute mass balance equation in an unstirred batch cell can be written as:

$$\frac{\partial C_j}{\partial t} = D_j \frac{\partial^2 C_j}{\partial z^2} + J(t) \frac{\partial C_j}{\partial z} \quad (3.27)$$

3.7.1 Species balance for the metal ions (j=1)

Considering the rate of removal of chromate ions due to adsorption on to the micelle surface, equation 3.28 is modified as follows:

$$\frac{\partial C_j}{\partial t} = Dj \frac{\partial^2 C_j}{\partial z^2} + J(t) \frac{\partial C_j}{\partial z} - \frac{K\rho_b}{M} \frac{\partial C_j}{\partial t} \quad (3.28)$$

where the term $\frac{K\rho_b}{M} \frac{\partial C_j}{\partial t}$ represents the sink term for the metal ion.

Rearranging the above equation, we get,

$$\frac{\partial C_j}{\partial t} = \frac{1}{\{1 + \frac{K\rho_b}{M}\}} \left[Dj \frac{\partial^2 C_j}{\partial z^2} + J(t) \frac{\partial C_j}{\partial z} \right] \quad (3.29)$$

The appropriate initial and boundary conditions are:

$$\text{at } t = 0, C_j = C_{j,b} \quad (3.30)$$

$$\text{at } z = 0, C_j = C_{j,b} \quad (3.31)$$

$$\text{at } z = \infty, J(C_{m,j} - C_{p,j}) = Dj \frac{\partial C_{m,j}}{\partial z} \quad (3.32)$$

Intrinsic rejection coefficient during MEUF may be defined as

$$R_{r,j} = 1 - \frac{C_{p,j}}{C_{m,j}} \quad (3.33)$$

3.7.2 Species balance for surfactant monomer (j=2)

A balance for total surfactant concentration as monomer in the aggregation layer can be easily obtained from equation 3.28.

The required initial and boundary conditions are:

$$\text{at } t = 0, C_j = C_{j,b} \quad (3.34)$$

$$\text{at } z = 0, C_j = C_{j,b} \quad (3.35)$$

$$\text{at } z = \infty, J(C_{m,j} - C_{p,j}) = Dj \frac{\partial C_{m,j}}{\partial z} \quad (3.36)$$

The intrinsic rejection coefficient for the surfactant monomer can be defined similar to the equation 3.34.

The observed rejection coefficient can be written as:

$$R_{obs,j} = 1 - \frac{C_{p,j}}{C_{b,j}} \quad (3.37)$$

As the membrane surface concentration is always greater than the bulk concentration, intrinsic rejection coefficient will be greater than the observed rejection coefficient.

It can be stated here that even though the surfactant monomer permeate concentration (C_{2p}) remains below CMC, the concentration at which the monomers are formed, the total surfactant concentration at the membrane surface may exceed the CMC value.

The following constraints are to be considered:

$$C_{2p} = (1 - R_r)C_{2m} \text{ if } C_{2m} < C_{CMC} \quad (3.38)$$

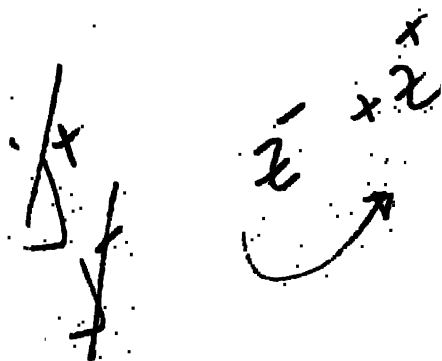
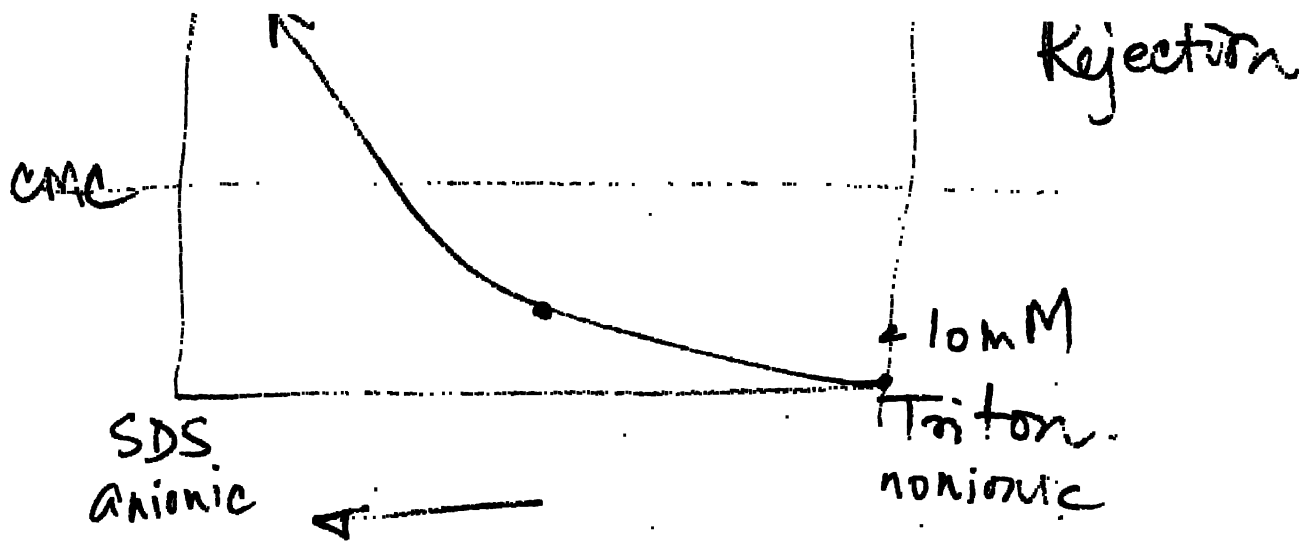
$$C_{2p} = (1 - R_r)C_{CMC} \text{ if } C_{2m} \geq C_{CMC} \quad (3.39)$$

3.7.3 Permeate Flux

The volumetric flux of the solution $J(t)$ can be expressed as:

$$J(t) = \frac{\Delta P - \Delta \pi}{\mu_s [R_m + R_{MAL}]} \quad (3.40)$$

where $\Delta \pi$ is the osmotic pressure difference of the surfactant monomer and μ_s is the viscosity of the aqueous solution.



Nomenclature

Symbols	Items	Units
a_1	Volume percentage of CO in top gas (dry)	(%)
a_2	Volume percentage of CO ₂ in top gas (dry)	(%)
a_3	Volume percentage of H ₂ in top gas (dry)	(%)
a_4	Volume percentage of H ₂ O in top gas (dry)	(%)
a_5	Volume percentage of N ₂ in top gas (dry)	(%)
a_1'	Calibrated vol. percentage of CO in top gas (dry)	(%)
a_2'	Calibrated vol. percentage of CO ₂ in top gas (dry)	(%)
a_3'	Calibrated vol. percentage of H ₂ in top gas (dry)	(%)
a_4'	Calibrated vol. percentage of H ₂ O in top gas (dry)	(%)
a_5'	Calibrated vol. percentage of N ₂ in top gas (dry)	(%)
a_1^s	Weight percent SiO ₂ in coal ash	(%)
a_2^s	Weight percentage Fe ₂ O ₃ in coal ash	(%)
A	Surface area of particles between level z and $z+dz$	(m ²)
A_c	Effective surface area of coke	(m ²)
A_1	Ash in coal	(%)
$(\%Ash)_{coke}$	Ash in coke	(%)
c_{pig}	Specific heat of i^{th} gaseous species	(cal/deg/mole)
c_{pis}	Specific heat of j^{th} specie of solid phase	(cal/deg/mole)
C_r	Boudourd reaction rate	(mol/cm ³ /sec)
C_{rg}	Carrier gas to coal ratio	(Nm ³ /kg)
C_1	Carbon in coal	(%)

4.1 Membrane and Chemicals

Membrane

Type : GR81PP; Danish Separation Systems, Denmark
Diameter : 76 mm
MWCO : 10,000
pH, Temperature, Pressure Range: 1 – 13, 0 – 75°C, 0 – 145 psi

Chemicals

- a) Sodium Chloride of purity 99.9% was procured from BDH, Mumbai.
- b) Cetyl Pyridinium Chloride [$C_{21}H_{38}ClN$] of purity 98% was obtained from Loba Chemie, Mumbai.
- c) Potassium Chromate of purity 99.0% was procured from Ranbaxy Ltd, India.

4.2 Instruments and other auxiliaries

UF Cell Specification

UF cell was designed and manufactured at the workshop in IIT, Kanpur.

Material of Construction : SS – 316
Total useful volume : 300 ml
Residual Volume : 100ml
Maximum Operating Pressure : 1000 kPa

Stirrer Characteristics

Diameter of the stirrer : 0.045m
Height of the stirrer
above the membrane : 0.03m

Stirrer Motor (Remi Motor, Mumbai) with range (Supply: 220V; Amperage: 0.6A;
Horse Power :0.05 Hp; RPM: 4000)

Compressor (Type: VDE 0530) with range (Supply: 220V, 1 Phase, 50 Hz;
Amperage: 2.6 A; Wattage: 180 W)

Tachometer

Model : Toshniwal hand tachometer, Type 630
Range : 30 to 50,000 rpm

Dialysis Cell

The cell was designed and fabricated at the workshop in IIT, Kanpur.

Material of Construction : Glass
Total Volume : 2 × 425 ml

Weighing Balance

Model : Afcoset Electronic Balance
Accuracy : 0.0001 g
Maximum Weight : 180 g

VIS – UV Spectrophotometer

Model : UV – 1601, Shimadzu Corporation, Japan

4.3 Solutions

Solutions of cetyl pyridinium chloride and chromate were prepared with 0.01 M sodium chloride in distilled water. The presence of salt decreases the CMC of ionic surfactants and thereby, reduces the loss of surfactant in the monomeric state.

4.4 Measurement of Density and Viscosity

The density of solutions was measured using specific gravity bottle at the ambient temperature. The viscosity was measured using an Ostwald viscometer at ambient temperature.

4.5 Design of Experiments

Experiments were designed to study the effects of applied pressure and feed concentration on the permeate flux and retention of surfactant. The flux and permeate concentration were measured at varying surfactant concentrations of 0.1 mM to

40 mM under stirred (stirrer speed:700 rpm) as well as unstirred conditions in a batch cell. The surfactant concentration was then held constant and the permeate flux and concentration was measured as a function of time for three different pressures (376 kPa, 580 kPa and 716 kPa).

The permeate flux and concentration of chromate solution was also measured as a function of time for the above three levels of pressures.

For adsorption studies, chromate concentration was varied from 0.1mM to 1.5 mM at constant surfactant concentration. The chromate concentration was then kept constant while the surfactant concentration was varied from 1 mM to 60 mM.

For semi – equilibrium dialysis (SED) analysis, chromate concentration was varied from 0.5 mM to 1 mM keeping surfactant concentration constant. Then chromate concentration was held constant while surfactant concentration was varied.

4.6 Experimental Procedure

A fresh membrane was placed on the porous support of the UF cell shown in the Fig.4.1. The cell was then assembled and filled with distilled water. Initial compaction of the membrane was carried out. For this purpose, the cell was pressurized using an air compressor and the flux was measured as a function of time. The operation was carried out at a pressure of 952 kPa for six hours. Constancy of water flux during this period suggested that no further compaction was necessary. The selected compaction pressure was higher than the highest operating pressure to ensure no compaction during the actual experimental work. For estimation of R_m the pressure was then varied and the flux was recorded as a function of applied pressure. The hydraulic membrane resistance was obtained from the linear relationship of pressure vs. flux data. To calculate flux, cumulative volume of water was collected in measuring cylinder and time for the collection was noted.

For experimental runs, the cell was dismantled and the membrane was rinsed with distilled water. The test solution was poured in the cell. It was pressurized and the permeate flux was measured at regular intervals. Permeate concentration of the surfactant and chromate was calculated from the absorption values using VIS – UV spectrophotometer.

After each run, the cell was rinsed with distilled water. The membrane was washed thoroughly and rinsed with distilled water. The water flux was measured after each run to check the loss of permeability of the membrane. For the stirred cell, the stirrer speed was measured using a tachometer.

In case of SED experiment, the membrane was presoaked with distilled water and thoroughly washed before use. A solution of CPC in NaCl containing known amount of potassium chromate was taken in one compartment of the dialysis cell and an aqueous solution containing same amount of NaCl was placed in the other compartment. The concentration of chromate and CPC in the permeate solution were analyzed as a function of time as above.

4.7 Measurement of Concentration

The optical density, being an extensive property is additive (provided there is no reaction between the solutes). Therefore;

$$A_{\lambda_1} = A_{1,\lambda_1} + A_{2,\lambda_1} \quad (4.1)$$

$$A_{\lambda_2} = A_{1,\lambda_2} + A_{2,\lambda_2} \quad (4.2)$$

where, A_{λ_i} is optical density at wavelength λ and the subscripts 1 and 2 refer to the two different wave lengths. The wavelengths are selected to coincide with the absorption maxima of the solutes. The absorption spectra of the two solutes should not overlap appreciably, so that substance 1 absorbs strongly at wavelength λ_1 and weakly at λ_2 . Whereas, the substance 2 absorbs strongly at λ_2 and weakly at λ_1 . We know $A_{\lambda} = a_{\lambda} \cdot C \cdot L$ (4.3)

where, a_{λ} is the molecular extinction co-efficient at any particular wave-length, C is the concentration expressed in gmoles per liter and L is the thickness (length) of the absorbing solution expressed in cm.

If L remains constant,

$$A_{\lambda_1} = a_{1,\lambda_1} C_1 + a_{2,\lambda_1} C_2 \quad (4.4)$$

$$A_{\lambda_2} = a_{1,\lambda_2} C_1 + a_{2,\lambda_2} C_2 \quad (4.5)$$

Solving the simultaneous equations, we get,

$$C_1 = \frac{a_{2,\lambda_2} A_{\lambda_1} - a_{2,\lambda_1} A_{\lambda_2}}{a_{1,\lambda_1} a_{2,\lambda_2} - a_{2,\lambda_1} a_{1,\lambda_2}} \quad (4.6)$$

$$c_2 = \frac{a_{1,\lambda_1} A_{\lambda_2} - a_{1,\lambda_2} A_{\lambda_1}}{a_{1,\lambda_1} a_{2,\lambda_2} - a_{2,\lambda_1} a_{1,\lambda_2}} \quad (4.7)$$

The values of the molecular extinction coefficient can be deduced from the measurements of the optical densities of pure solutions of substances 1 and 2. By measuring the optical density of the mixture at wavelengths λ_1 and λ_2 , the concentrations of the two components can be calculated. In our experiment, cetylpyridinium chloride is represented as substance 1 and chromate solution as 2.

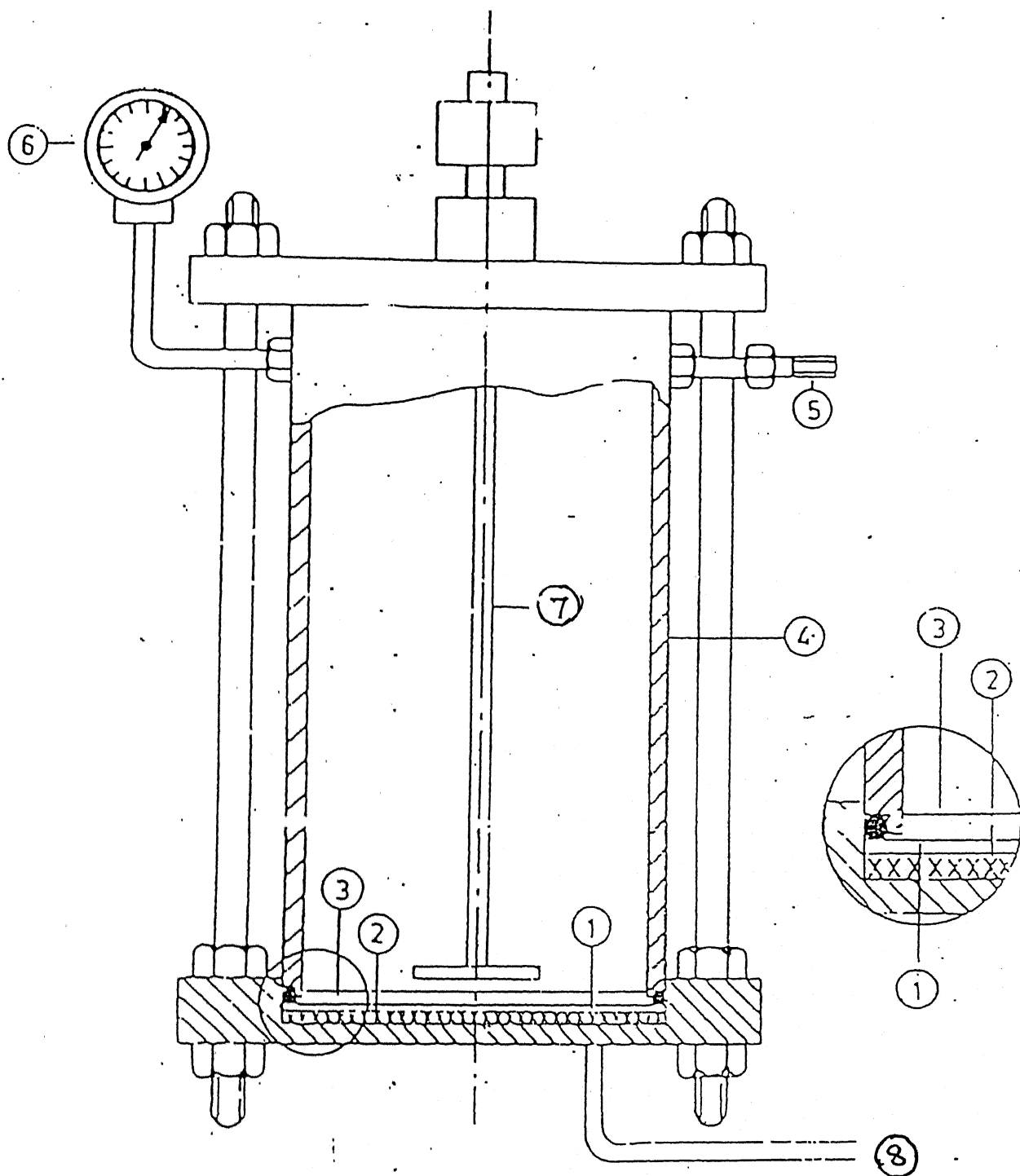


Fig. 4.1 Ultrafiltration Cell

1. Membrane 2. Porous Support 3. 'O' Ring 4. Cell Body 5. Pressure line Connector 6. Pressure Gauge 7. Stirrer 8. Sample Outlet

Chapter 5

Results and Discussion

Micellar enhanced ultrafiltration studies were conducted for the removal of chromate ions from aqueous solution. The objective is to specifically study the effects of operating conditions, such as pressure and concentration of both CPC and chromate, on the permeate flux, surfactant rejection and chromate rejection.

5.1 Selection of Operating Conditions

As seen from equation 3.15 flux depends on the difference between the applied pressure and the osmotic pressure. However, osmotic pressure is negligible in case of CPC as the micelles formed are of considerable size. A concentration, as high 180 kg/m^3 of CPC, exerts an osmotic pressure of around 210 kPa [4]. To obtain flux at measurable level, the operating pressure range was kept on the higher side and was varied from 376 to 716 kPa .

The micelles of CPC form at a critical concentration of 0.88 mM . The concentration of feed CPC was varied from 0.1 to 0.5 mM to study the behaviour of CPC below CMC. Whereas, the feed CPC was varied up to 40 mM for the studies of concentration beyond CMC. This helped us to study the behaviour of CPC when it falls below CMC during MEUF, unlike having to study removal of chromate ions in presence of micelles.

The chromate concentration was varied from 0.1 mM to 1.5 mM . Beyond this limit, the permeate concentration of chromate is way above that of standard wastewater norms which is 0.1 g/m^3 for inland water disposal [6].

Hexavalent chromium remains in solution as $[\text{CrO}_4]^{2-}$ and as $[\text{HCrO}_4]^-$. Hence, anionic surfactant cannot be used in the present case. The solubilisation as well as the adsorption capacities of the nonionic surfactants are not high compared to the ionic surfactants. Hence, it was decided to carry out experiments with cationic surfactants which infact give advantages in terms of low Krafft temperature and possibility of the formation of large micelles. Cetyl pyridinium chloride, a cationic surfactant, was used as it has a large hydrophobic group with the Krafft temperature of 10.8°C . Therefore, it can be used effectively at room temperature.

5.2 Micellisation and Ultrafiltration of Surfactant Solution

Effects of pressure as well as concentration of the surfactant on permeate flux and surfactant rejection were studied. The surfactant concentrations were varied from 0.1 to 0.5 mM (below the CMC) and from 10 to 40 mM (above CMC). Permeate flux and concentration were measured and analyzed as a function of time. The experiments were conducted and the values were recorded until not much appreciable change was observed. Such values (obtained almost constant) will now be henceforth referred as final values.

Effect of pressure on permeate flux and surfactant rejection

The effects of pressure were observed on permeate flux by applying three different pressures. Fig 5.1 depicts the flux variation with time using 30 mM surfactant solution at three different pressure levels. It was observed that the flux remains constant with time. This shows that the effect of concentration polarization is negligible; otherwise a decline in the flux would have been observed. This is being reiterated as the experiments were carried out under unstirred condition, there could have been a possibility of the partial blockage of membrane pores by micelles and/or a formation of an additional resistant layer. Micellar Aggregation Layer (MAL) may have declined the flux. However, on plotting final value of flux with applied pressure (Fig 5.2), the linear relationship was not observed beyond 580 kPa. Although, minutely observed, the decline in flux was observable. Therefore, it may be concluded that at high pressure there seems to be effect of concentration polarization.

Fig 5.3 depicts the fall of CPC rejection values as a function of time. As the time progressed, the retentate total (bulk + micelles) concentration of CPC increased. Since the bulk concentration maintains at CMC level extra CPC monomers further grow into separate micelles or increases the size of already existing micelles. Thus, the resistance of MAL increases and retention of such micelles increases. Further, this effect is more pronounced as the pressure is in the lower region. At higher pressures, these micelles may break into dimers and trimers, which may permeate through and therefore experience lower rejection.

However, an observation shown in Fig 5.2 also depicts a variation of final value of surfactant rejection with pressure. Since the surfactant concentration was much higher than the CMC (around 34 times), the rejections were not found to vary much with pressure (see inset of Fig.5.2). Whereas, in the expanded form of rejection values, Fig.

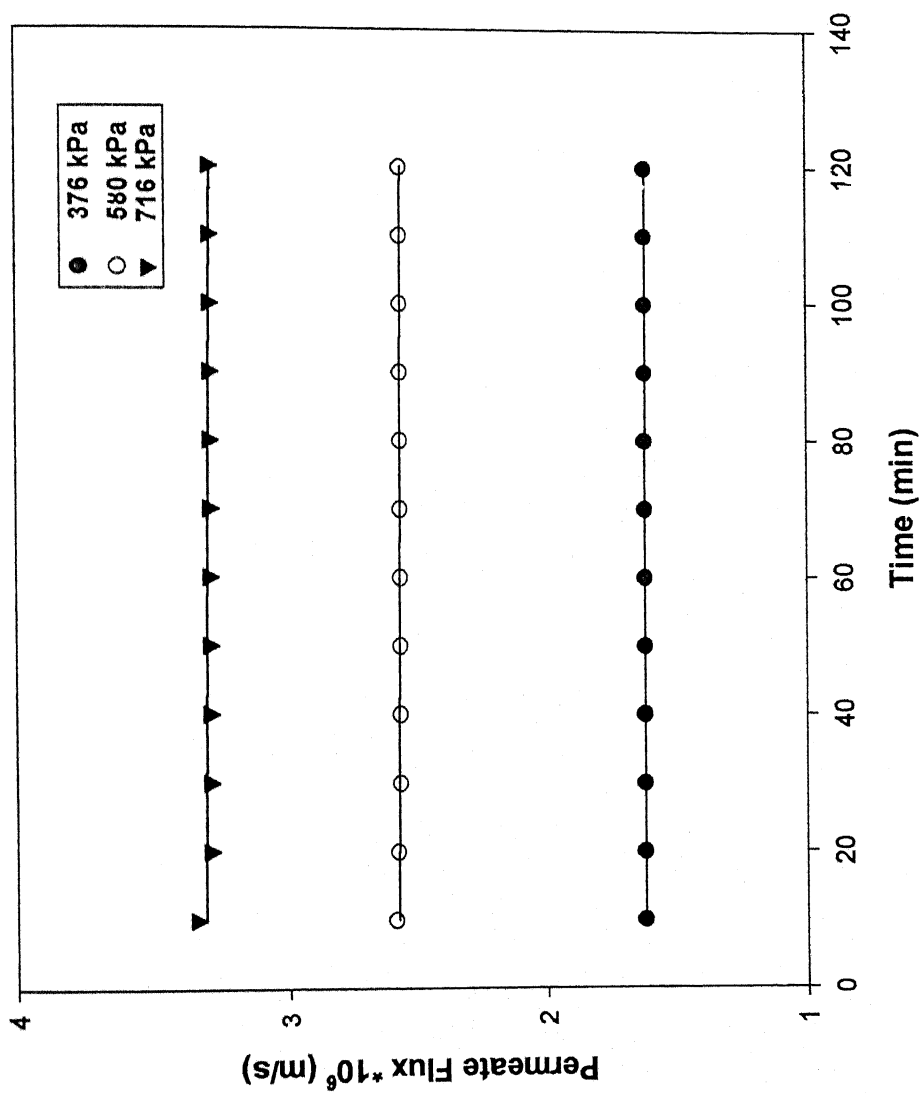
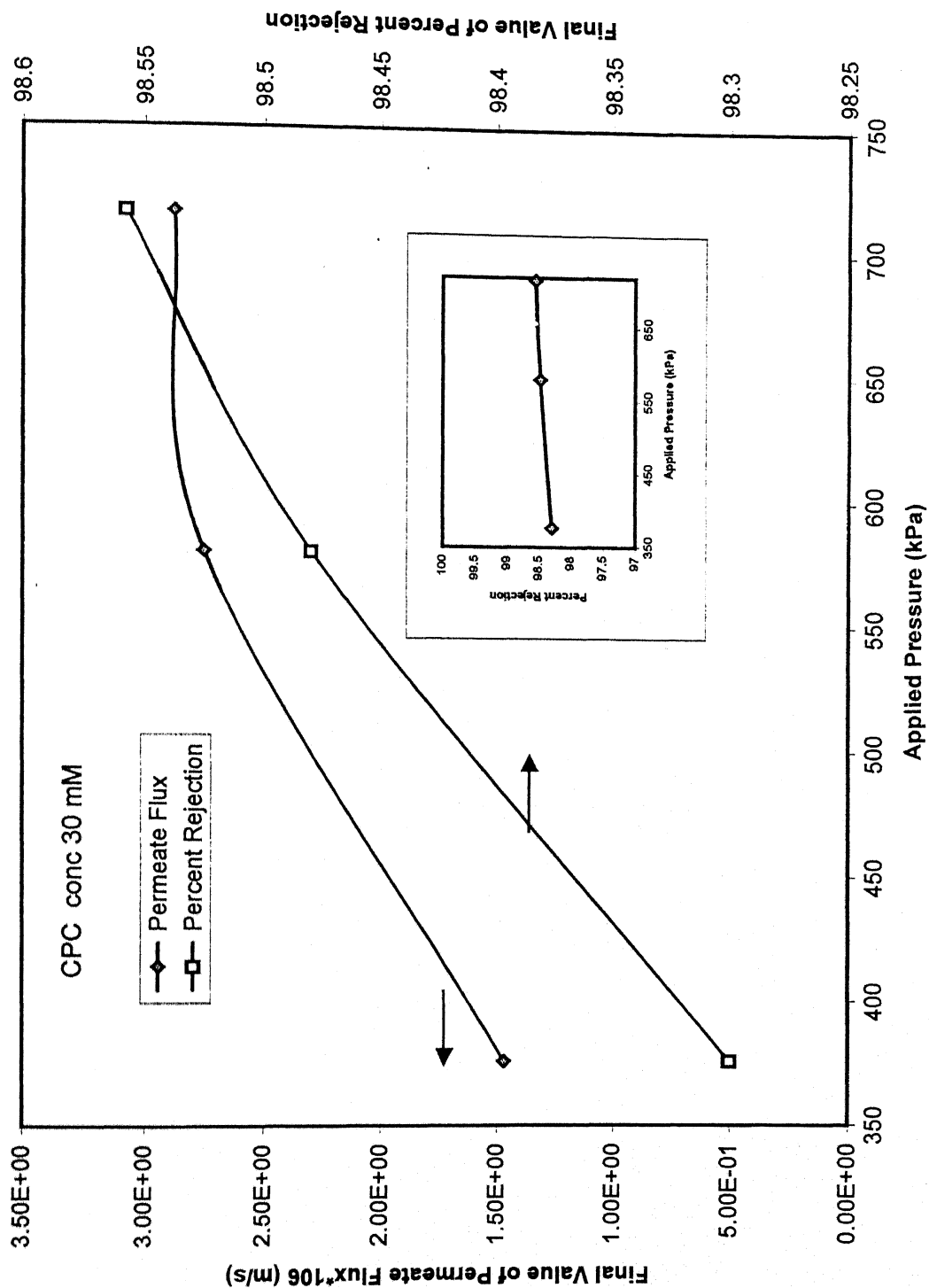


Fig.5.1 Variation of CPC [30mM] permeate flux with time

Fig.5.2 Permeate Flux and CPC Rejection vs Applied Pressure



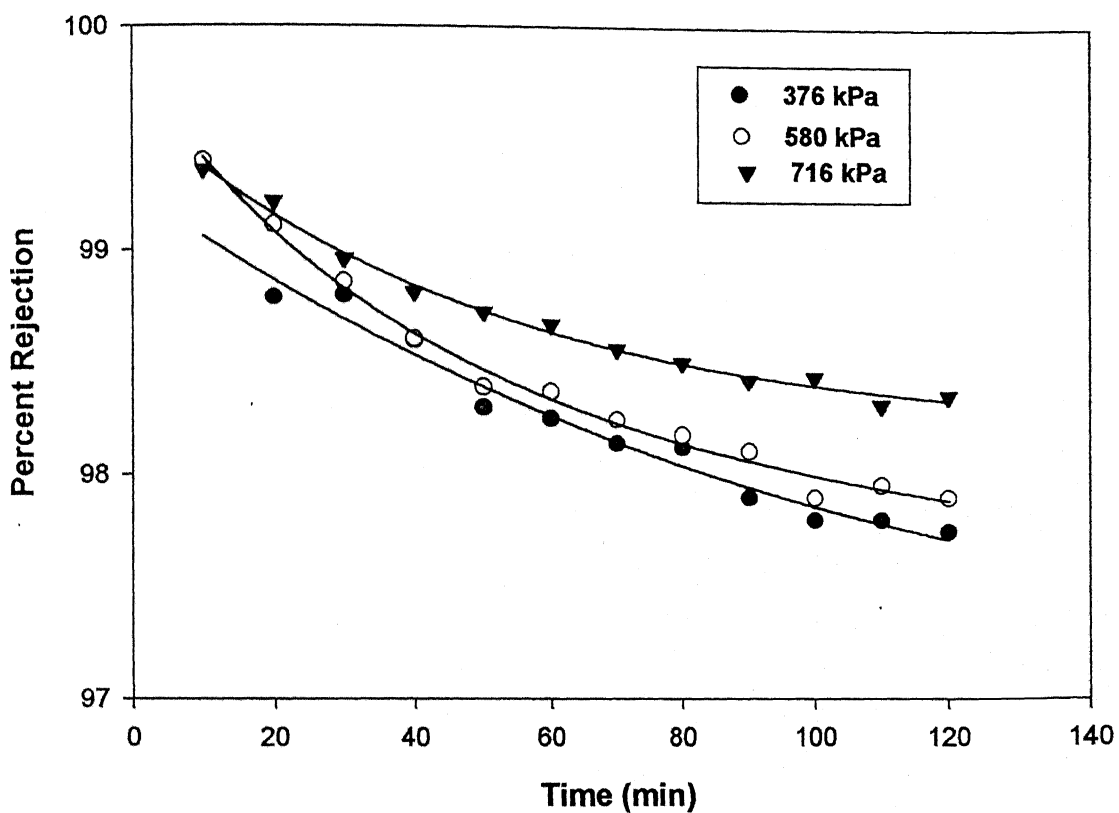


Fig. 5.3 Percent Rejection vs Time plot of 30 mM CPC soln.

5.2, a trend was observed. It was found that the rejection increases with the increase in applied pressure. This may be attributed to the formation of the additional layer, called Micellar Aggregation Layer (MAL), on the surface of the membrane at such high concentrations. This layer provides an additional resistance to the solvent flow and deters the passage of free surfactant through the membrane. This phenomenon is severe at high pressures due to compaction of the aggregation layer.

Effect of feed surfactant concentration on permeate flux and surfactant rejection

To observe the influence of CPC concentration below CMC, a plot was made between percent rejection and time and shown in Fig. 5.4. It may be observed that the trends of curves are similar to that obtained with CPC concentration above CMC. However, the percent rejections were found to be much less; particularly as the time progresses. This is because all the surfactant molecules are in the form of free monomers, the size of which is much smaller than the pore diameter of the membrane used (MWCO-10,000). Other authors have reported similar trends [7]. However, any rejection of the free surfactant molecules may be due to the adsorption of these molecules on the membrane surface.

The final values of permeate flux variation as a function of feed surfactant concentration in Fig. 5.5 reveal that the permeate flux exponentially decreases. The present case, therefore, seems to be governed by resistance-in-series model. Such interpretations are based on the concentration polarization layer on the membrane or the secondary membrane, which induces transfer resistance [6]. With the increase in surfactant feed concentrations, larger fraction of micelles are formed. Hence, the MAL thickness increases; as a result the resistance offered by this increases and consequently the permeate flux declines. The reduction in the permeate flux may be also due to the partial coverage of the membrane pores by these micelles. This effect increases with the increase in feed concentration.

In an attempt to observe the range of feed CPC concentration for MEUF, a plot was made between permeate CPC and feed CPC concentration, which is shown in Fig. 5.6. It is evident from the figure that beyond a feed concentration of 43 mM (critical feed concentration, CFC), the permeate concentration increases beyond CMC value. The rapid rise in permeate concentrations sets the limit for the maximum operational feed concentrations. This may be explained due to the breaking of micelles into dimers and trimers that they are able to permeate through the membrane. Therefore, it

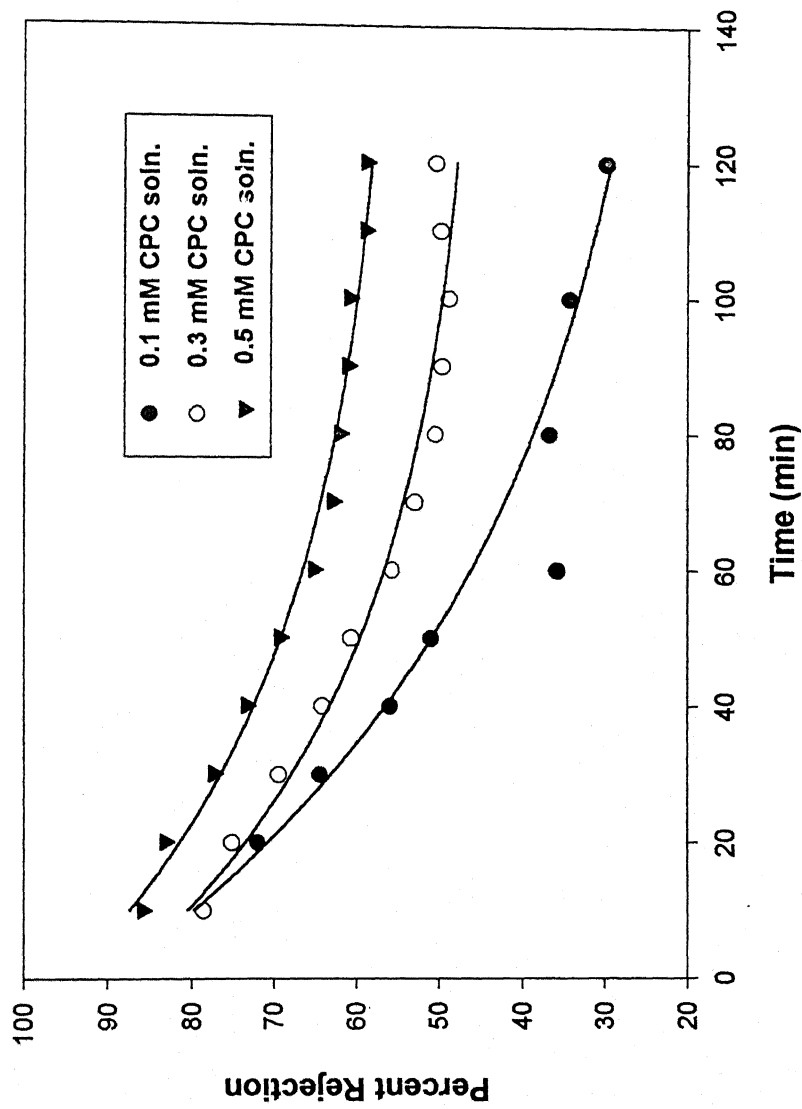


Fig.5.4 Percent Rejection vs Time plot at 580kPa

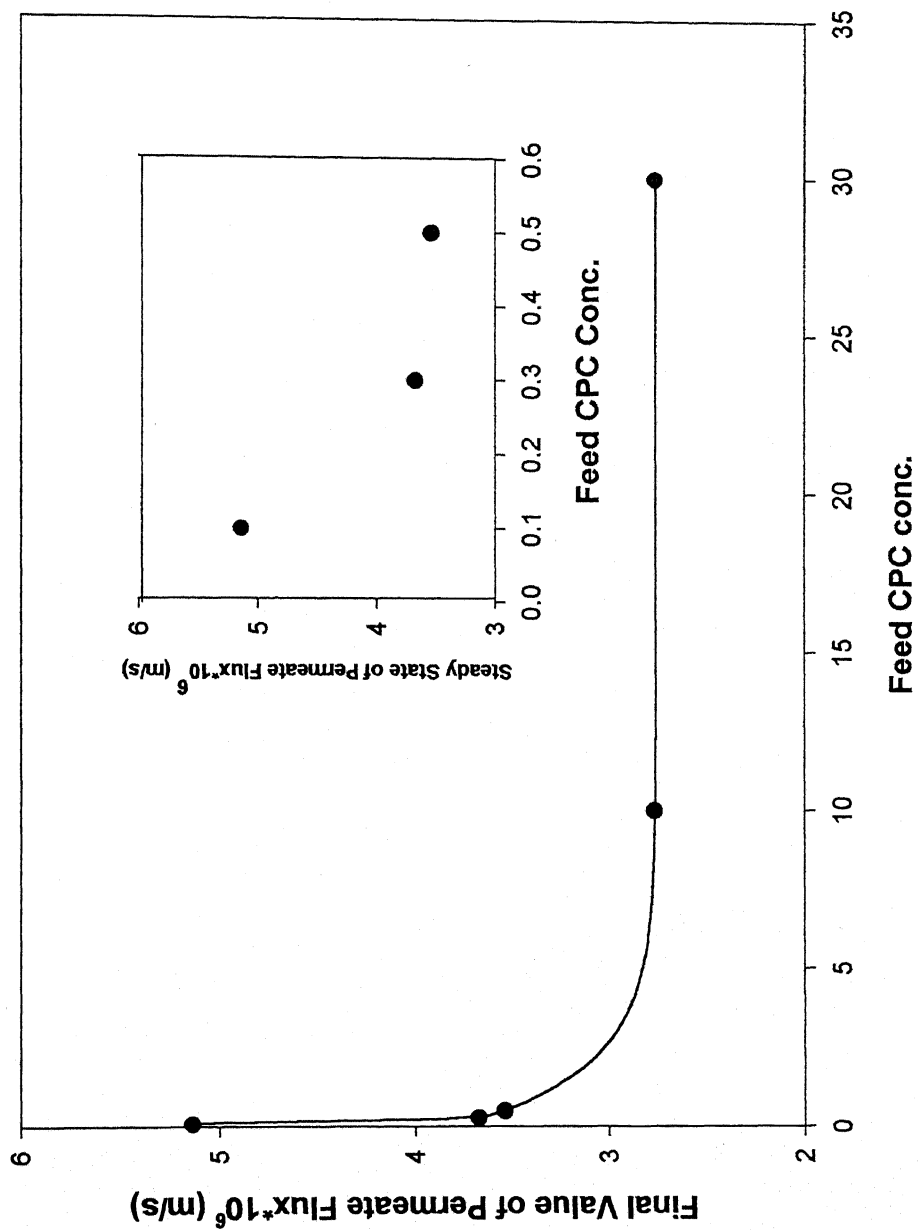


Fig.5.5 Permeate flux vs Feed CPC Conc at 580 kPa

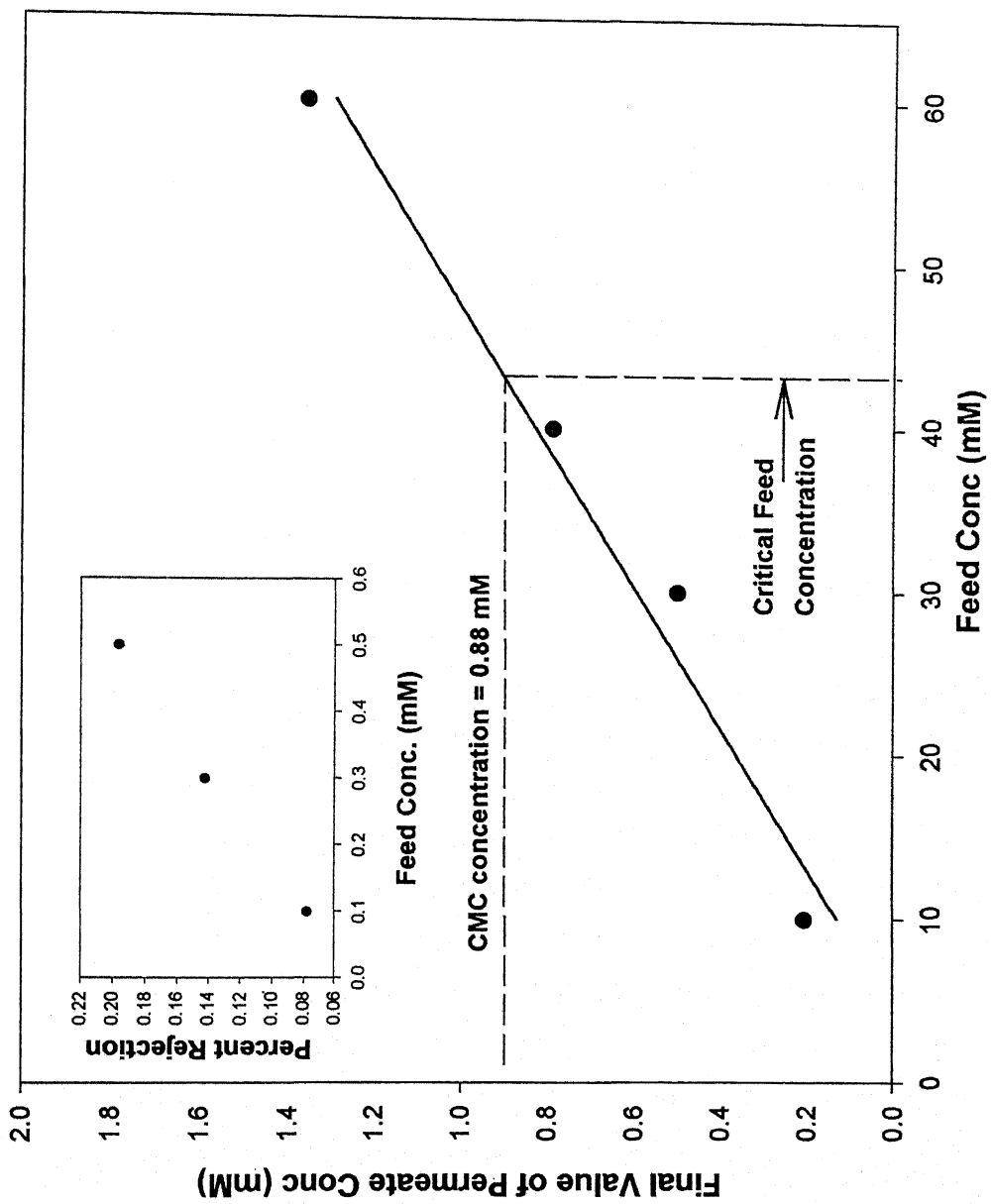


Fig. 5.6 Permeate Conc vs Feed Conc at 580 kPa

may be concluded that the feed CPC concentration should be well below CFC. However, Fig.5.7 depicts an immediate rise in rejection with the increase in feed CPC concentration which later on attains a plateau at higher CPC concentration. Comparing figures 5.6 and 5.7, it seems that to reject CPC at highest possible level as well as to avoid breakage of micelles, the feed CPC concentration should be in the range of 10 to 30 mM.

Effect of Stirring

At low feed concentrations, stirring aids the diffusion of monomer away from the membrane surface. Thus stirring helps in reducing the concentration gradient. As a result the permeate concentration is much low compared to that obtained for unstirred cell. Therefore, the percent rejection is higher in case of stirred condition than when experiments were carried out without stirring. This is illustrated in the Fig. 5.8.

5.3 Ultrafiltration of Chromate in absence of Surfactant

It was thought appropriate to observe the behaviour of the percent rejection as well as the permeate flux of chromate solution alone which is in other words, ultrafiltration of chromate solution in absence of CPC. Fig 5.9 and Fig.5.10 show the percent flux and the permeate retention of chromate solution respectively as a function of time at three different pressures. Although negligible effect of concentration polarization, there is a clear evidence of it with respect to increase in pressure as observed in Fig.5.9; particularly during the initial period of ultrafiltration. Likewise, from Fig.5.10, it is evident that there is a distinct drop in percent rejection during the initial period. This is because of initial adsorption of chromate with the polymeric membrane.

Fig 5.11 represents the variation of the hexavalent chromium rejection and permeate flux as a function of applied pressure for an initial chromate concentration of 50ppm. The plot shows that the rejection of chromate anions in water decreases from 10.5 to 3% with the increase in pressure from 376 to 716 kPa. Such a low rejection values suggest that there may be little adsorption of chromium on the membrane surface and most of it permeate through the membrane. The permeate flux is found to vary linearly with pressure which indicates there is practically no development of resistance against flow at such a low value of chromate concentration in feed.

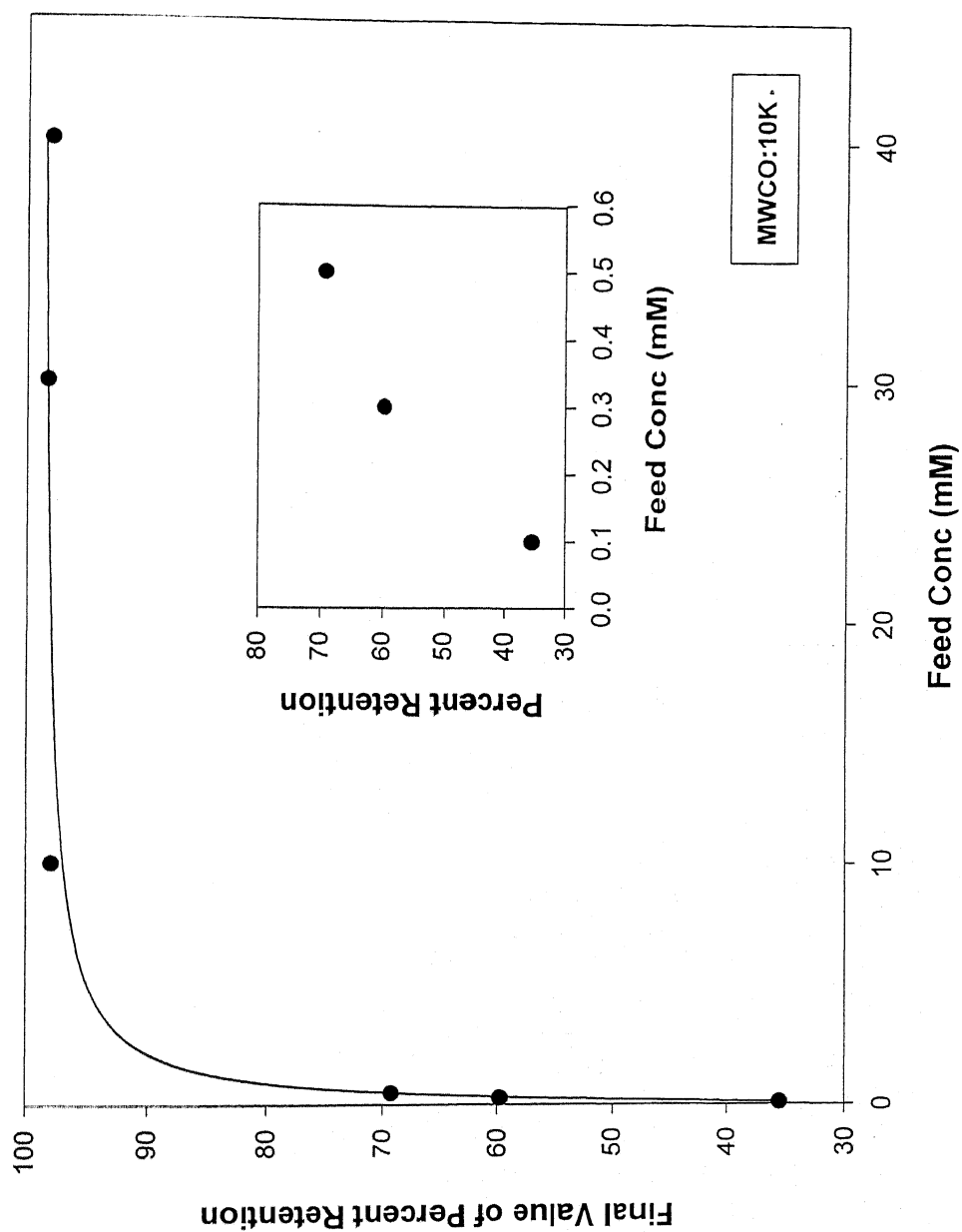


Fig.5.7 Percent Retention vs Feed Conc(mM) plot at 580 kPa

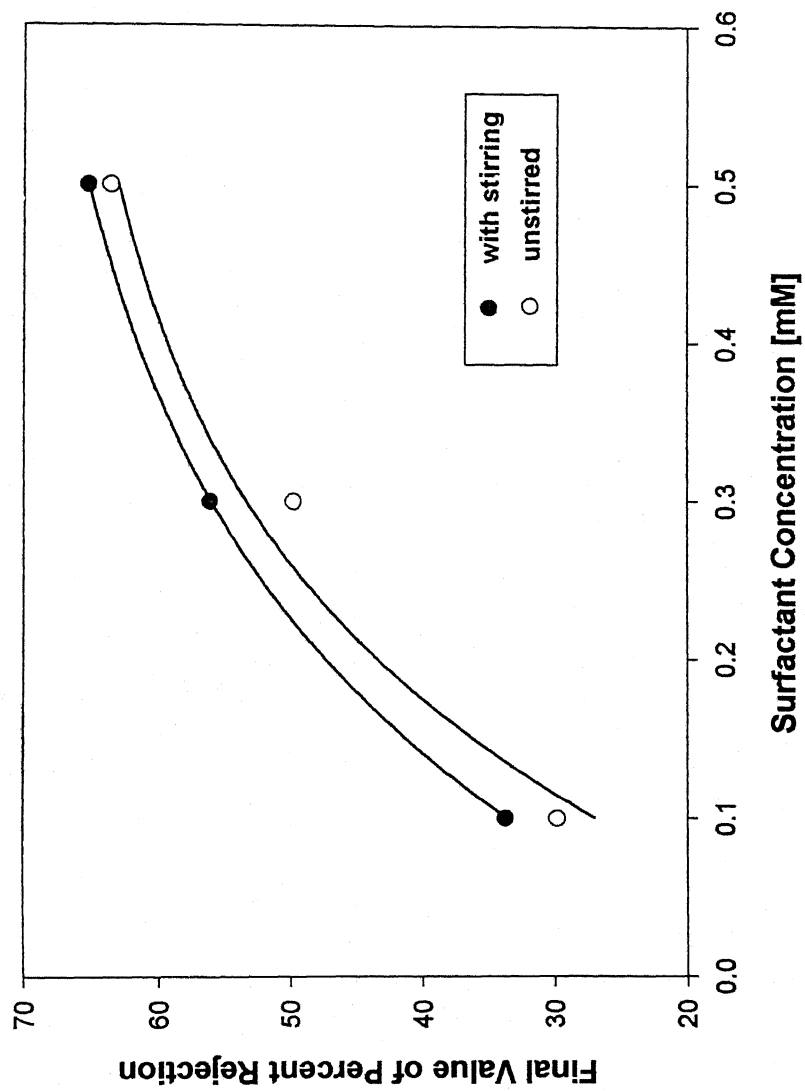


Fig. 5.8 Plot of Percent Rejection vs Surfactant Conc. at 580 kPa

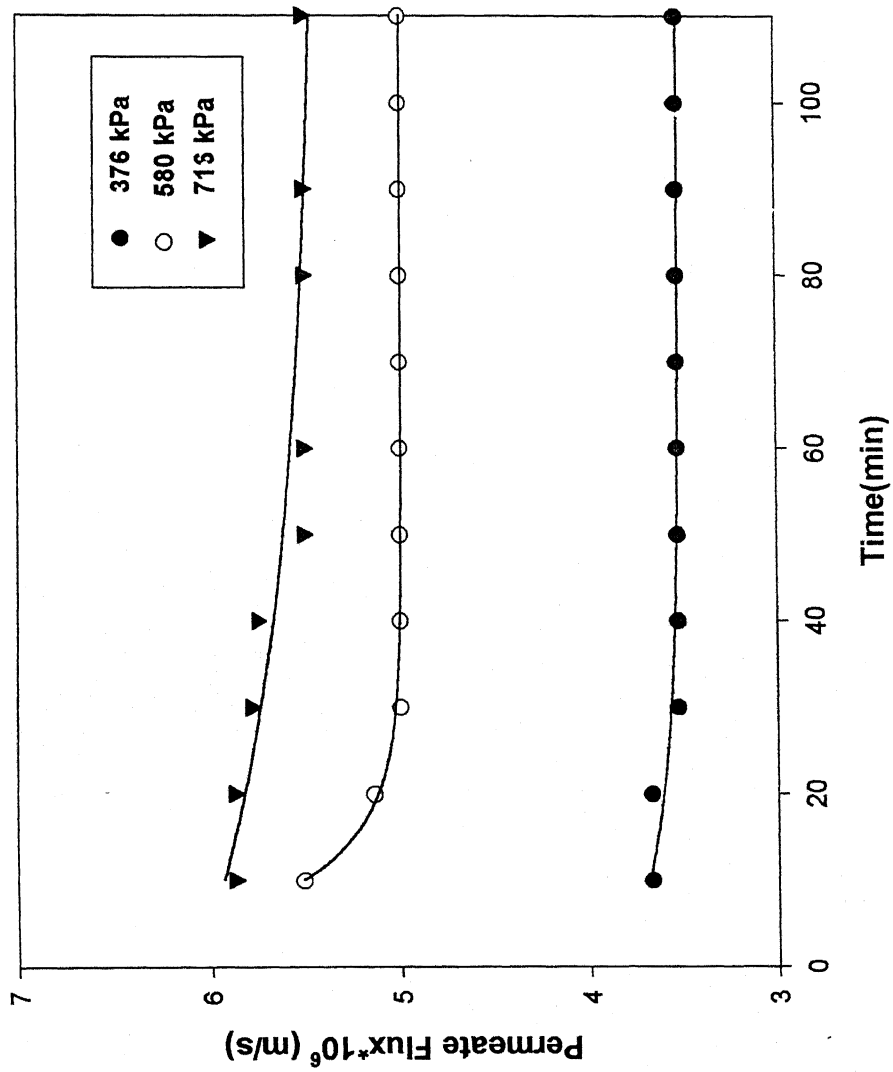


Fig.5.9 Permeate Flux Vs Time Plot for 50ppm Chromate soln.

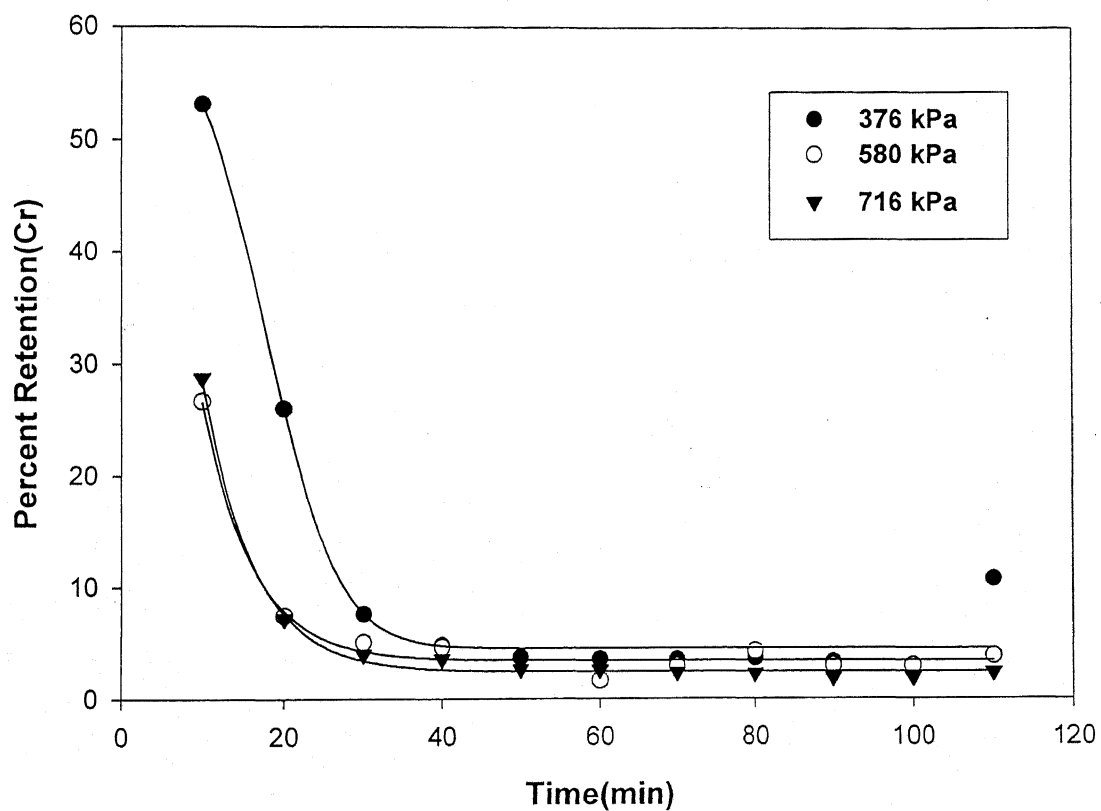
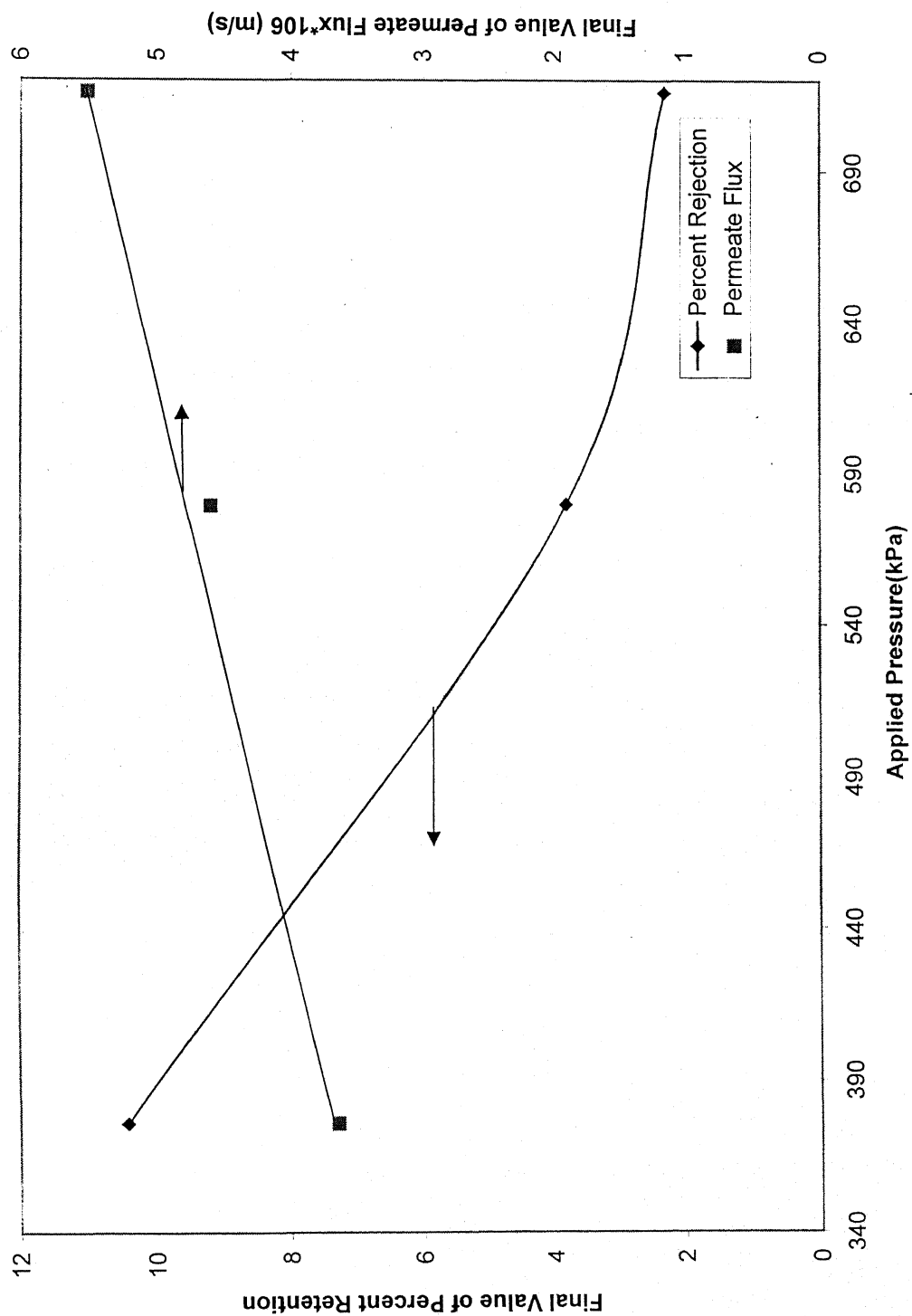


Fig.5.10 Percent Retention vs Time plot of 50 ppm Chromate soln

Fig.5.11 Percent Retention & Permeate Flux of Chromate solution (50 ppm) as a function of Applied Pressure



5.4 Separation of Chromate using Surfactant Solution

In this part of the work, the experiments were carried out with the surfactant and the metal ion. The solutions containing both of them were prepared for UF. The pH of the solutions was found to be around 6.5 for all the concentration of chromate ion in the CPC solution. It is known that at this condition of pH the chromate ion exists in the form of $[\text{CrO}_4]^{2-}$ as well as $[\text{HCrO}_4]^-$ in the solution. The effects of feed surfactant concentration, metal ion concentration as well as the effect of pressure on the permeate flux and chromate adsorption on the micelles (measured in terms of retention during UF) were studied.

Effect of chromate concentration

A plot in Fig.5.12 of permeate flux at varying chromate concentration as a function of time is made keeping the feed surfactant concentration constant (30mM). These curves depicts that the permeate flux more or less remains constant over the time range, indicating concentration polarization to be negligible. However, on minute observation there is an evidence of linear decline in flux (eg. 2.0×10^{-4} (m/s)/s for 0.3 mM concentration and 9.17×10^{-4} (m/s)/s for 0.7 mM chromate concentration). The decline is so little that a trend with chromate concentration could not be observed. Further, with the increase in chromate concentration there is a distinct decrease in permeate flux. Fig. 5.13 shows the influence of chromate concentration on flux. It is clearly evident that at higher chromate concentration the decline in flux is comparatively less. Further some authors [6] had stated that this may be due to the formation of mixed micelles. Chromate ion replaces the chloride ions from the micelles. With the increase in the metal ion concentration, the fraction of micelles containing chromate ions increases. As the size of chromate ion is greater than the chloride ion, the micelles formed of pure surfactant is smaller than that containing the metal ions. These bigger size metal ion containing micelles develop greater resistance for permeate flow and hence the flux decreases.

Fig.5.14 shows the percent rejection of chromate ions as a function of time, while varying its feed concentration. These curves depict one thing in common that the percent rejection initially increase, attains a maximum and then drop as a function of duration of UF for all the concentration of feed concentration of chromium. Further they all attain very high rejection (99.9%) values; however, differing with their

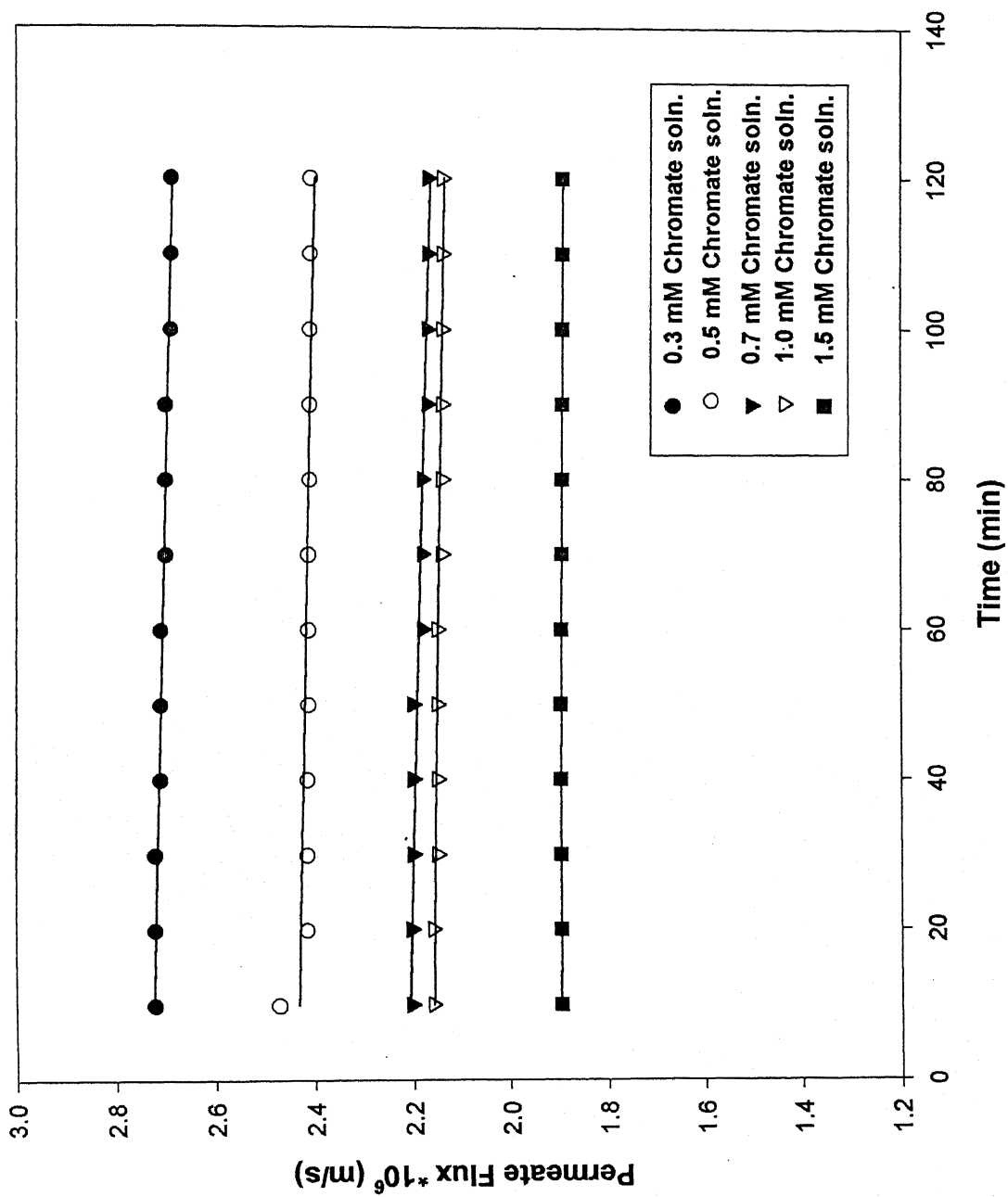


Fig. 5.12 Variation of permeate flux as a function of time with $[CPC] = 30 \text{ mM}$

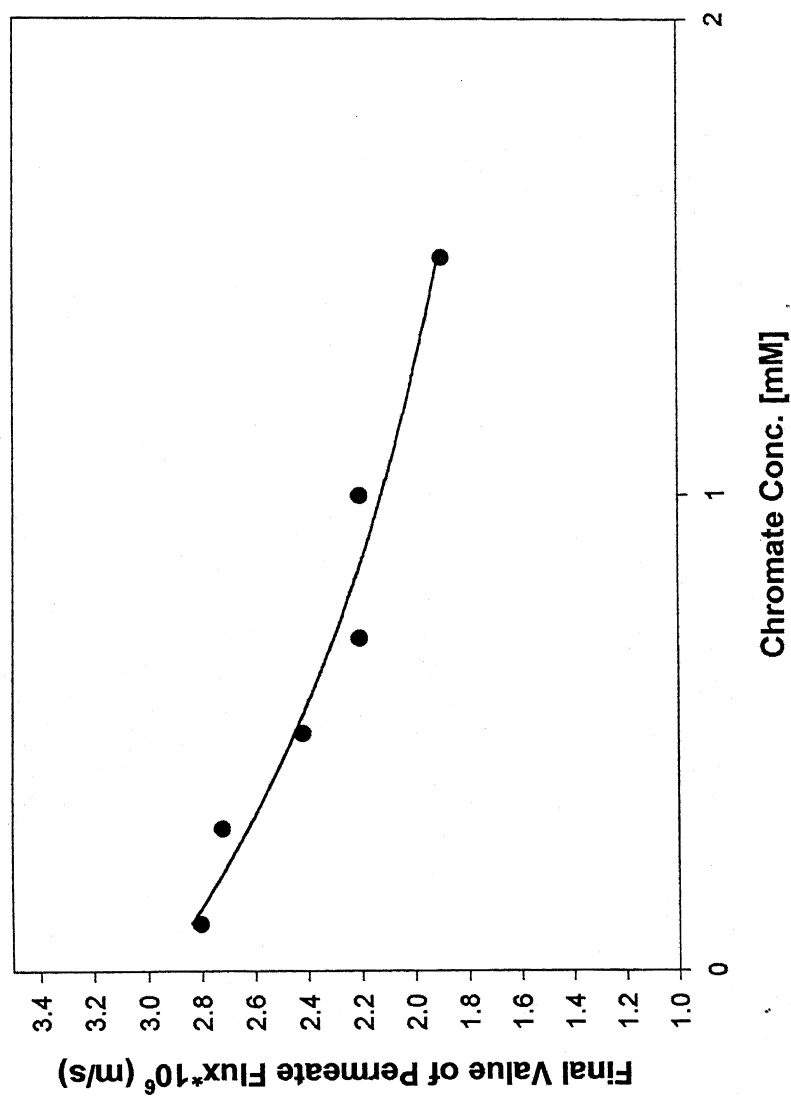


Fig. 5.13 Permeate Flux as a function of chromate concentration

पुरुषोत्तम काशीनाथ केलकर पुस्तकालय
भारतीय प्रौद्योगिकी संस्थान कानपुर

अवधि क्र० A-141945

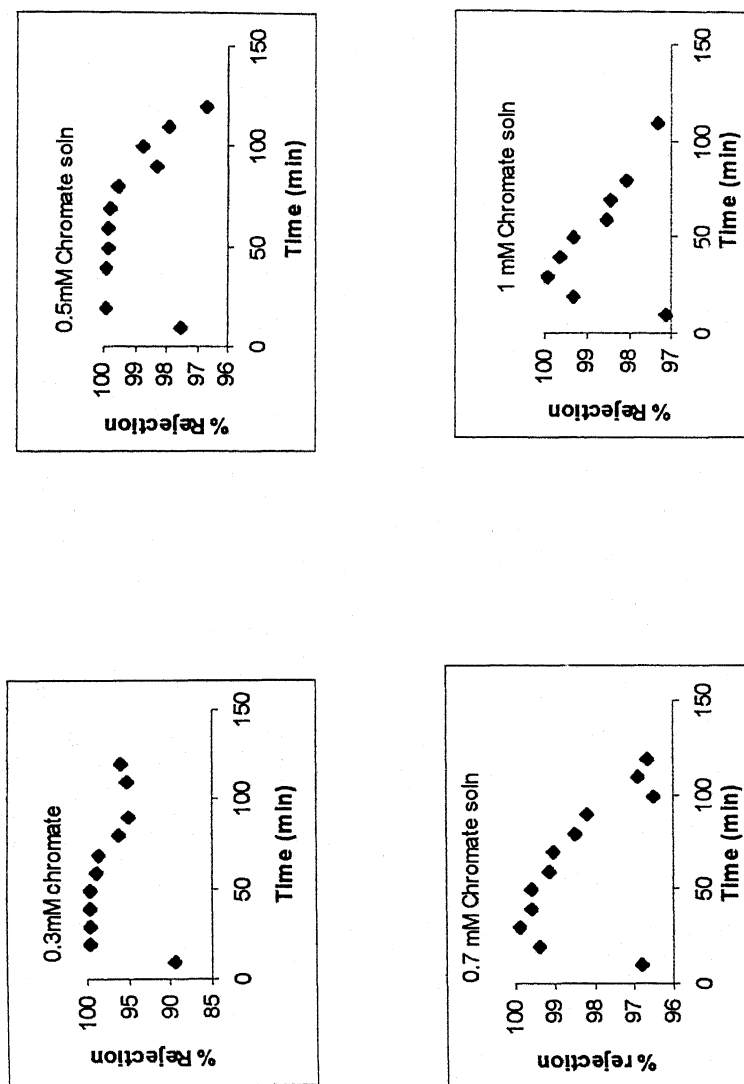


Fig. 5.14 Variation of Percent Rejection as a function of time at $[CPC] = 30 \text{ mM}$

duration of attainment. Since, there was no clear trend observed for the duration of attainment of maximum rejection, a separate plot was not made.

Effect of surfactant concentration

Fig. 5.15 shows the negligible influence of concentration polarization, as the permeate flux was observed to be invariant with time in presence of chromate ions for all concentration values of CPC; the explanation of which has been given earlier for runs with only CPC. Further, Fig.5.16 shows the decline in the final value permeate flux with increase in feed CPC concentration. This decline is marginal in the lower concentration range and increases at the higher concentration range. Obviously, this is due to the increased resistance of MAL against flow. Fig.5.16 further, depicts a significant increase in final values of rejections against increase in feed CPC concentration which then at higher range of concentrations steadily decline. The initial significant chromium rejections are due to the formations of more and more micelles. Authors [7] are having the idea that two opposite effects come into play at this situation which leads to a nearly constant permeate concentration even with increase in surfactant concentration. However, on increasing the surfactant concentration, micelle mole fraction increases and more chromate ions get entrapped. But at very high surfactant concentration, the ratio Cr(VI)/Cl decreases. As a result chloride ions get preferentially adsorbed on the micelle surface and the chromate concentration in the bulk increases. Hence, at a higher surfactant concentration the percent rejection decreases. This therefore slightly decreases percent rejections at higher concentrations.

Fig. 5.17 shows the percent rejection plot as a function of time for varying CPC concentration. The rejection increases initially with time and then there is a drop in percent rejection. This may be due the fact that with increase in CPC concentration the mole fraction of micelles being increased the rejection also increased. However, as the micelles break into dimers and trimers the percent rejection falls.

Effect of Pressure

The effects of pressure on permeate flux as well as on percent retention were studied. It was observed that transmembrane pressure did not have any significant effect on permeate concentration of chromate over the experimental range. Chromium rejection depends mainly upon the available amount of micelles, adsorption on the surface of

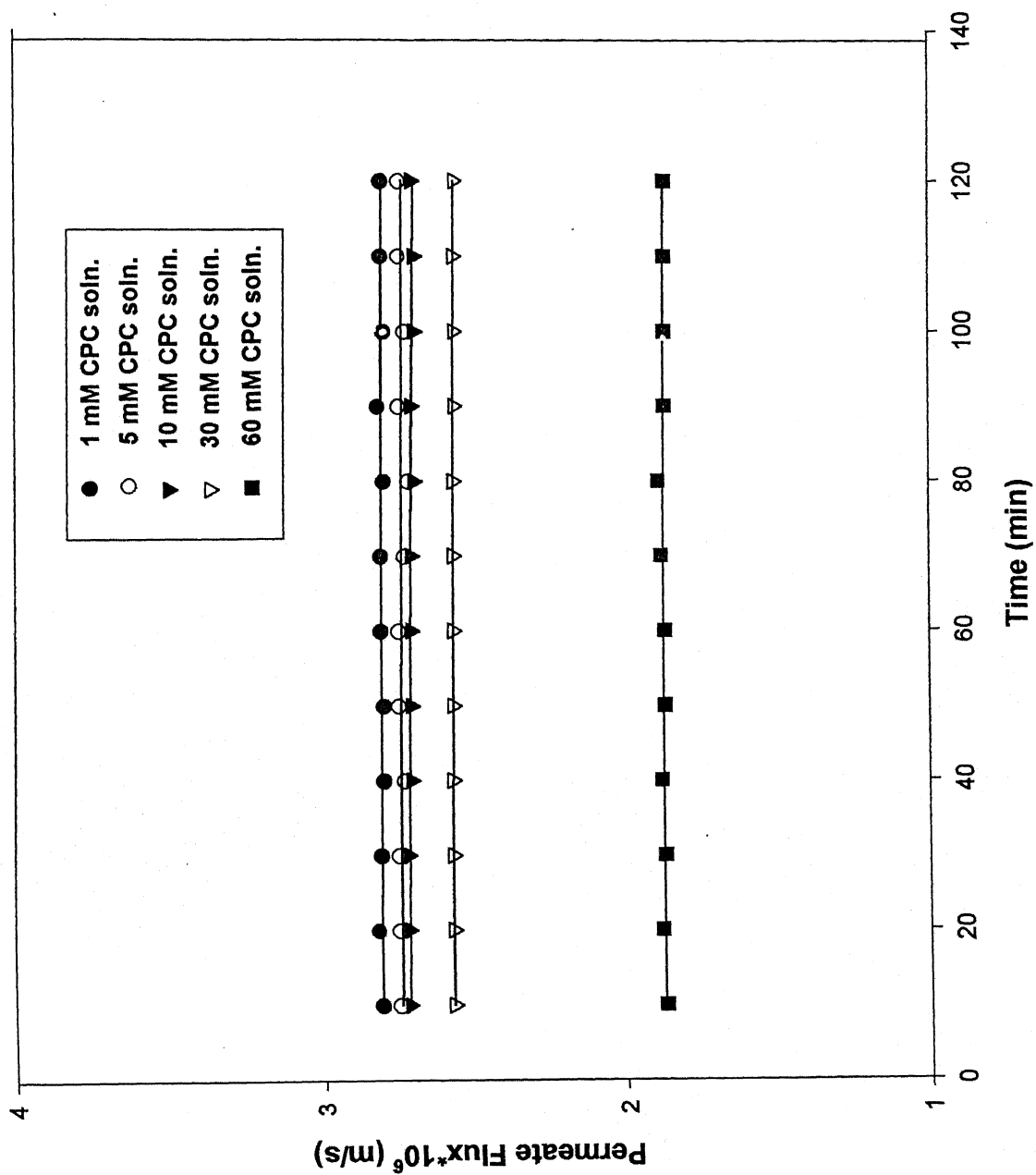
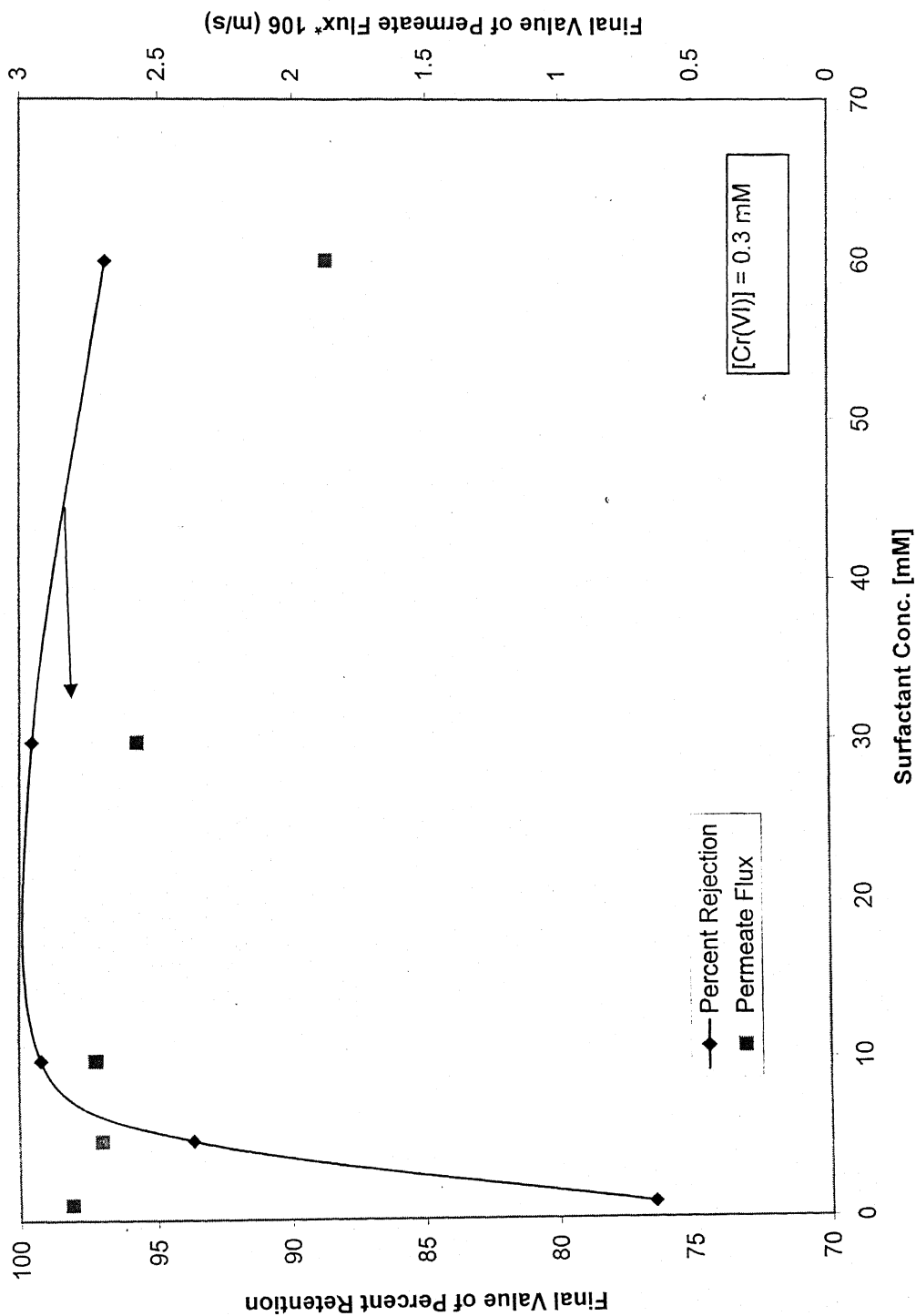


Fig.5.15 Variation of permeate flux with time at $[\text{Cr(VI)}] = 0.3 \text{ mM}$

Fig. 5.16 Percent Chromate Retention and Permeate Flux as a result of surfactant concentration



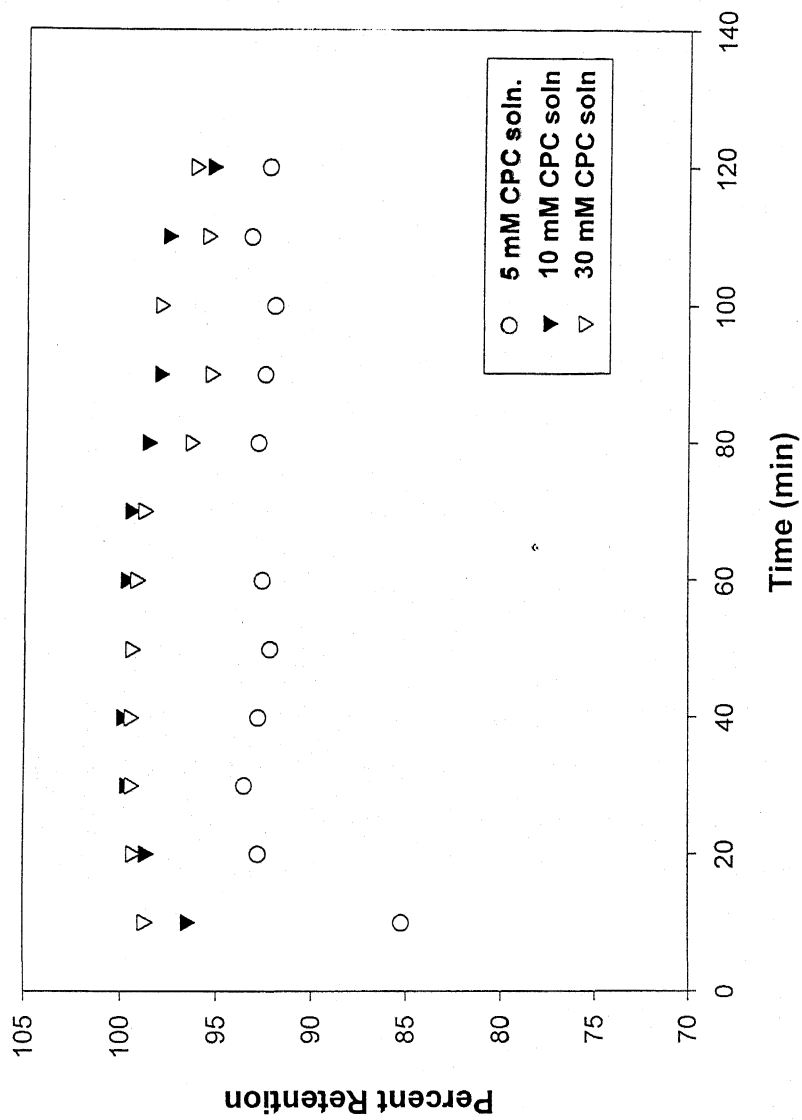


Fig. 5.17 Variation of Percent Retention with time at $[\text{Cr(VI)}] = 0.3 \text{ mM}$

the membranes as well as its own concentration. Since, in the present case, both chromium and feed CPC concentration (available amount of micelles) are constant, the only place of difference is adsorption on the membrane surface. Therefore, the pressure influence of the chromium adsorption on the membrane surface (with its concentration and feed surfactant concentration being constant) is being found negligible. However, if the pressure keeps on increasing, such adsorption on the membrane may clog pores and may show slight decline which is evident in Fig. 5.18 at higher pressures. However, the permeate flux was found to change linearly with the pressure, as shown in Fig. 5.18. Obviously, as has been shown earlier, there was no observance of concentration polarization, the expected linear trend was observed.

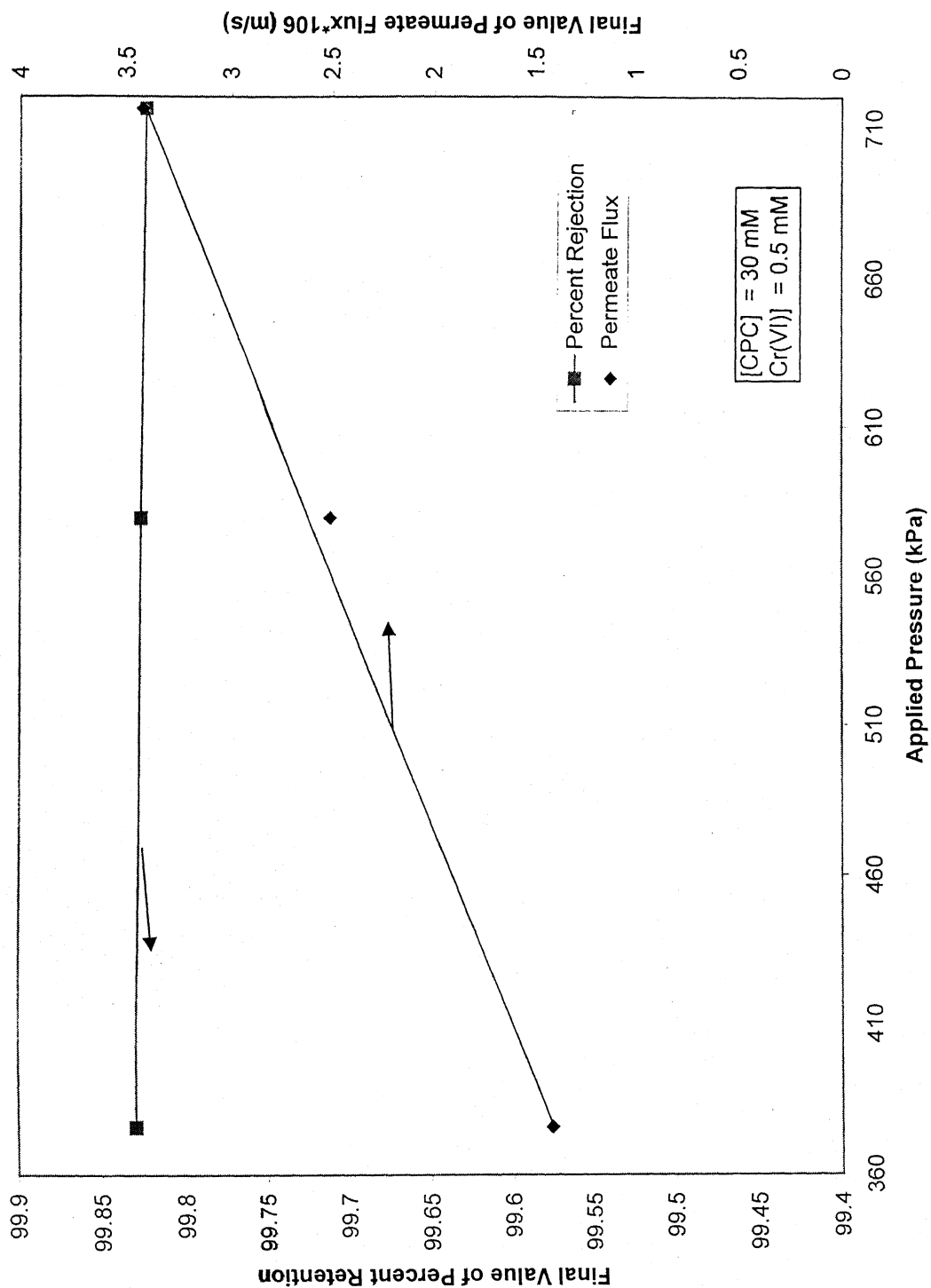
Adsorption

In MEUF, it is now assumed that the permeate concentration of chromate is equal to the unadsorbed chromate concentration in the retentate as well as adsorbed chromate on membrane surface (considered to be negligible, which is indeed very small). Therefore, the value of adsorbed chromium concentration and consequently the adsorption equilibrium constant K_f , when measured using MEUF were found slightly overestimated (as neglecting membrane adsorption portion).

The adsorption equilibrium constants were found out as shown in Fig. 5.19 according to the equation 3.21. Such values would be utilized later in the modeling section. However, the influence of feed surfactant concentration and chromium concentration on adsorption of chromium was observed and shown in Fig. 5.20. This plot is in effect would be giving similar trends as obtained with rejections versus feed CPC concentrations. Obviously as explained earlier the adsorption of chromate decreased with the increase in surfactant concentration. This is because with the increase in surfactant concentration the mole fraction of micelles also increases. Larger amount of adsorbing sites being present for the chromate, the adsorption of chromate per unit mass of micelles decreases.

The adsorption equilibrium constant calculated using semi-equilibrium dialysis method is much more accurate. Such experiments have also been performed; however, K data utility is required with phase wise modeling. Such work is in progress. Data have been however, provided in Appendix D.

Fig. 5.18 A plot of Percent Retention and Permeate Flux as a function of applied pressure



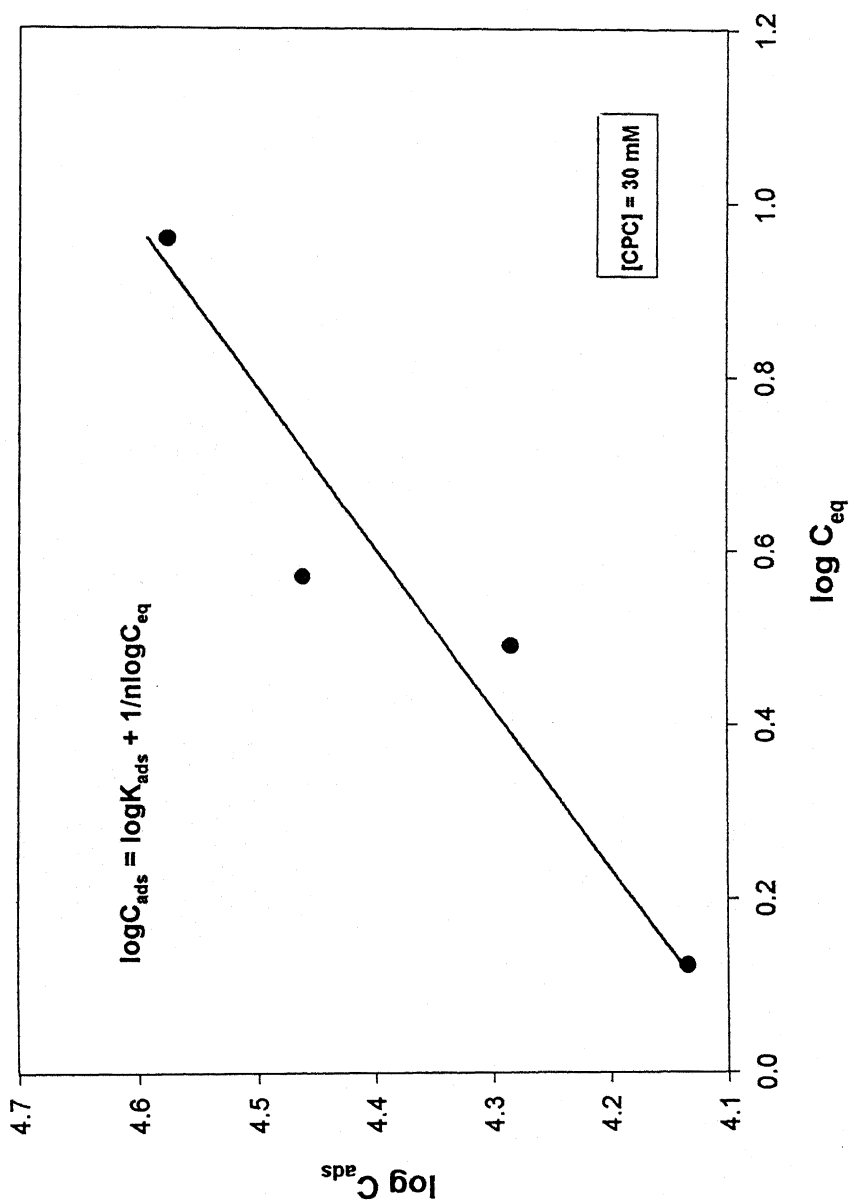


Fig. 5.19 Freundlich plot for the adsorption of Cr(VI) on the micelle surface

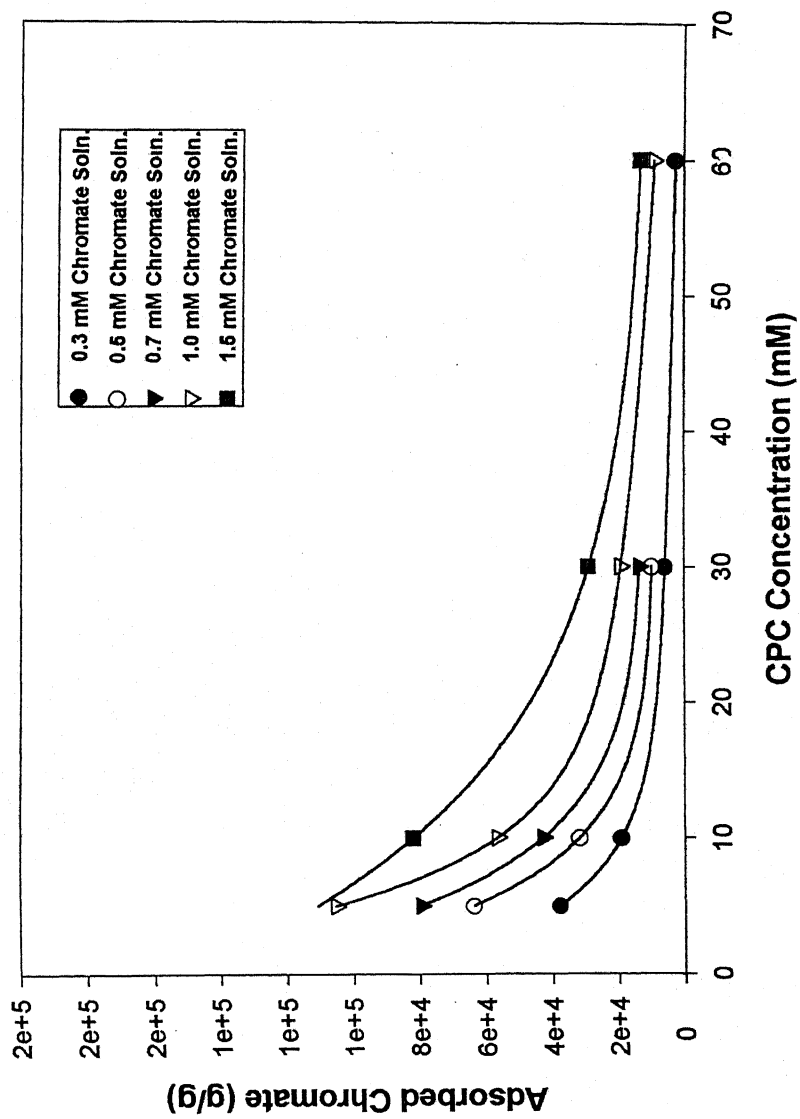


Fig 5.20 Adsorbed Chromate vs Surfactant Concentration

5.5 Analysis of results through developed model

A mathematical model was developed in Section 3.7 to predict the permeate flux and its concentration. Equations 3.27 and 3.29 were solved numerically using the respective initial and boundary conditions. The solutions were obtained using *NAG* subroutines (D03PDF of *NAG* Software library).

It was an important objective of the work to not only observe the predicted trends of permeate flux and its concentration, it was also to observe and examine certain influences of chosen parameters on the effectiveness of MEUF for the removal of chromate ions. Keeping in mind such objectives, model equations were reoriented in terms of some parameters (dimensionless) for better understanding of the process. In this approach, the first most common plot was made between permeate flux and time as shown in Fig. 5.21. As observed, there is an excellent matching between experimental data and predicted values. Similarly, Fig. 5.22 also shows close matching between permeate flux and applied pressure.

A plot, shown in Fig. 5.23, was made to depict the effect of permeate concentration (C_p/C_b) as a function of time (J^2t/D). Since, in this case C_b was fixed as CMC value of CPC (an assumption for the model development), it was expected that there would be a time where C_p/C_b would reach the value of one. However, such a time could not be observed, not only through experiments also through predicted values (as this would have taken much extrapolated values). Therefore, predicted as well as experimental values may be considered to be of close matching. Likewise, when a plot, shown in Fig. 5.24, was drawn for similar relationship, however along with chromium, the results were a bit different compared to blank CPC runs. Predicted values also show similar values and trends. Explanations have been provided earlier. Therefore, this may also be concluded as a close match.

Blank experimental runs with chromium ions were also predicted and good agreement was observed, as shown in Fig. 5.25. However, when runs of chromium adsorption on CPC micelles were predicted, as shown in Fig. 5.26, a good matching could not be achieved. This may be due to the fact that the model was developed on the basis of constant K value, which may not be the case in actual operation. This may change as a function of time. Therefore, semi equilibrium dialysis experiments are needed where K values may be obtained under different concentrations. Work is in progress.

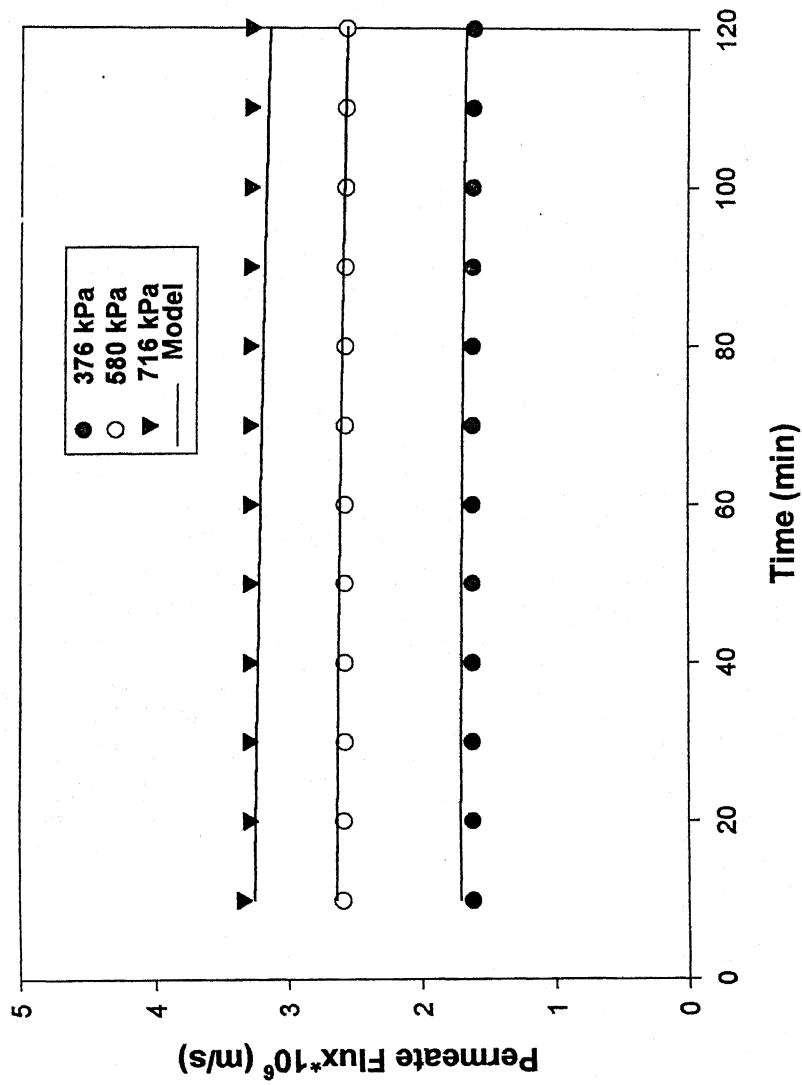


Fig.5.21 Variation of Permeate flux of CPC [30 mM] with time during MEUF

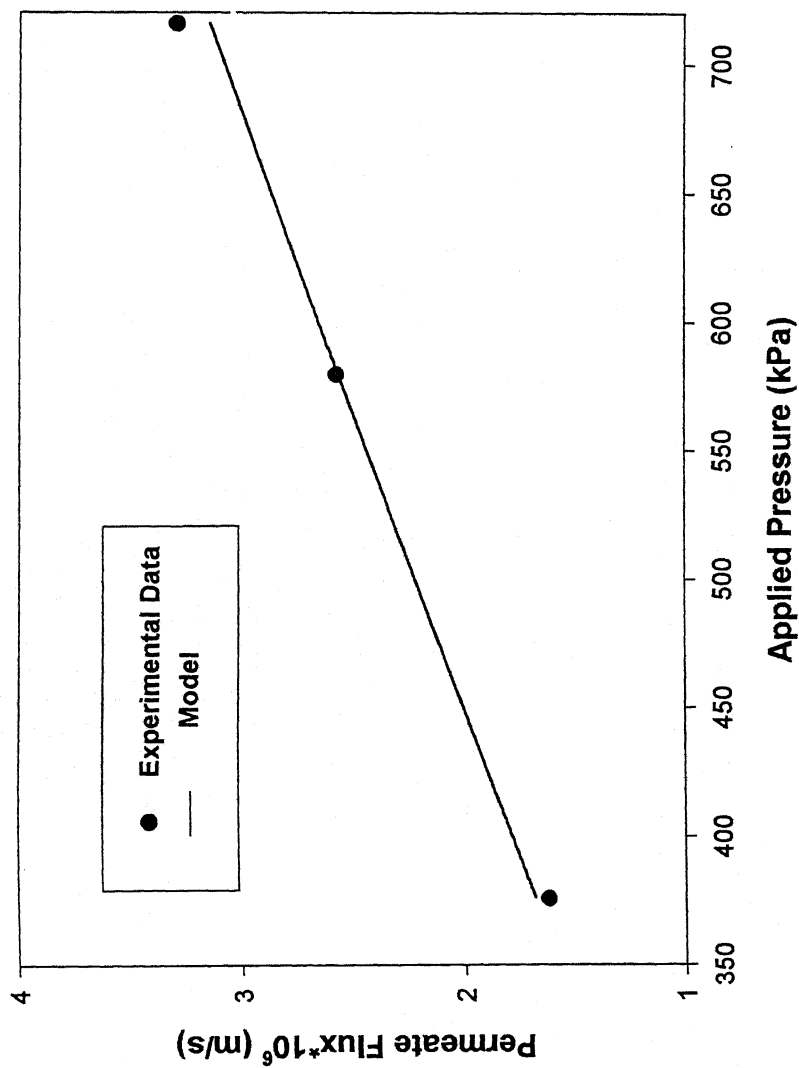


Fig.5.22 Permeate Flux of CPC (30 mM) as a function of Applied Pressure (kPa)

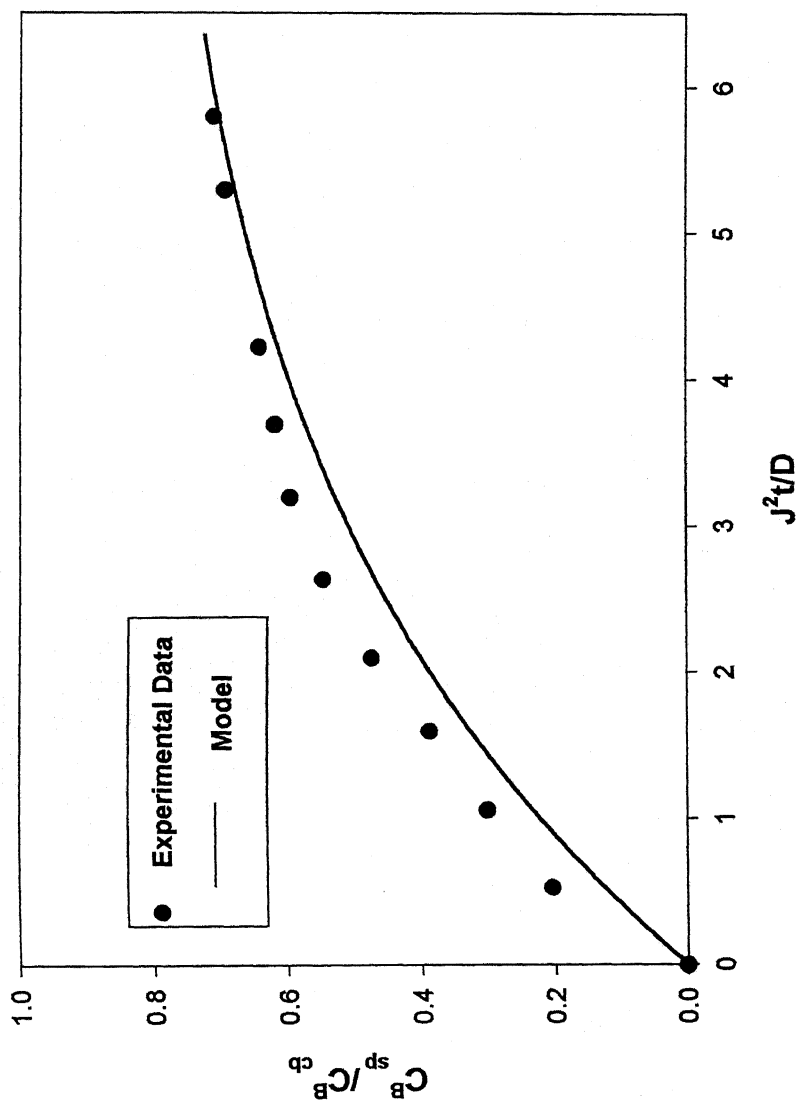


Fig.5.23 Variation of CPC [30 mM] permeate concentration with time during MEUF

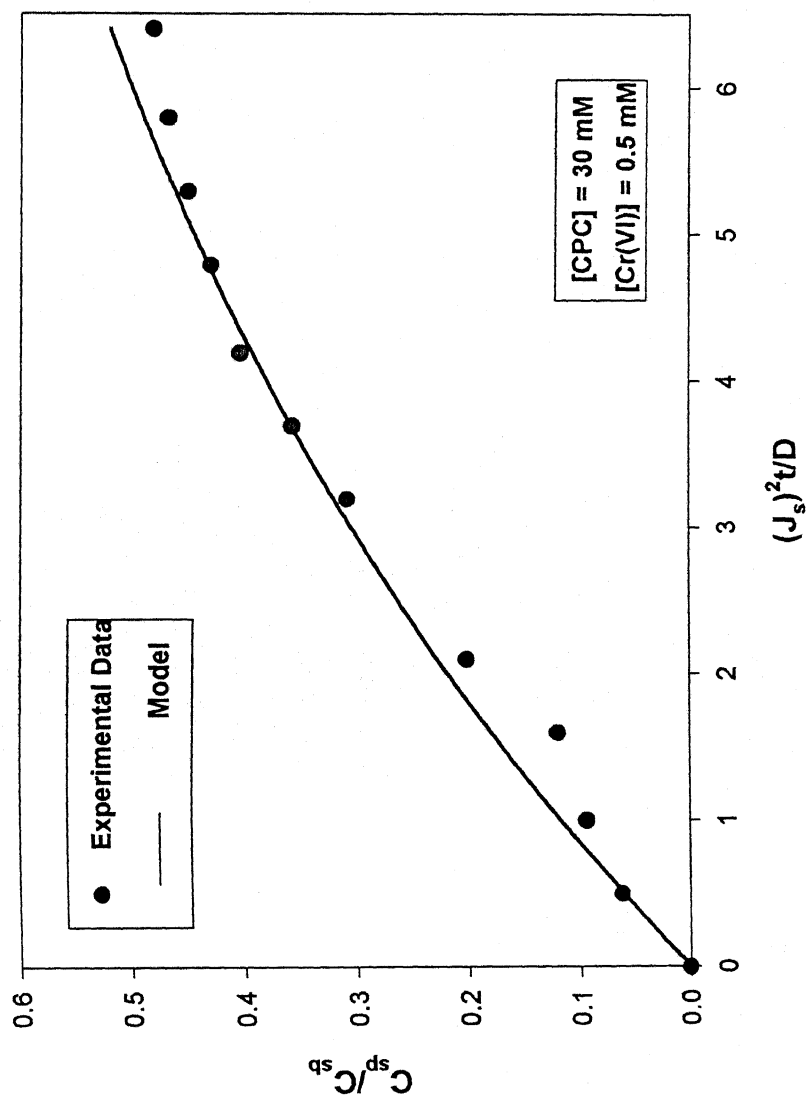


Fig.5.24 Variation of CPC permeate concentration with time during MEUF

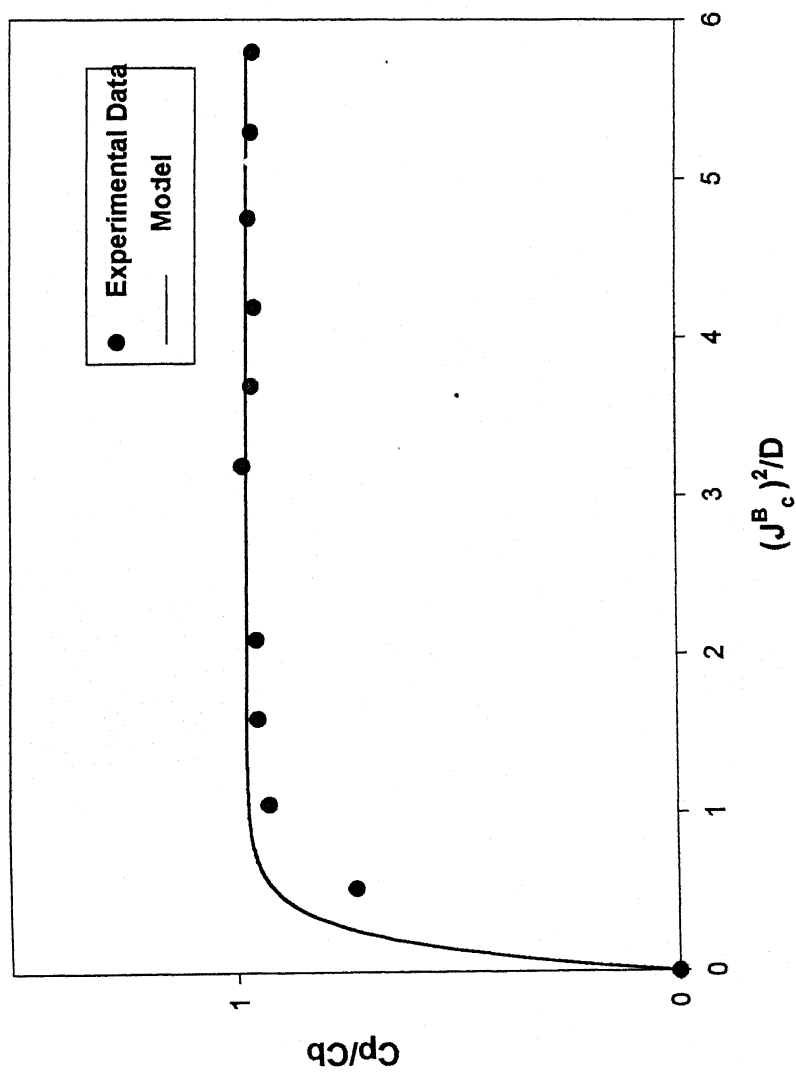


Fig. 5.25 Variation of Chromate (50 ppm) permeate concentration with time

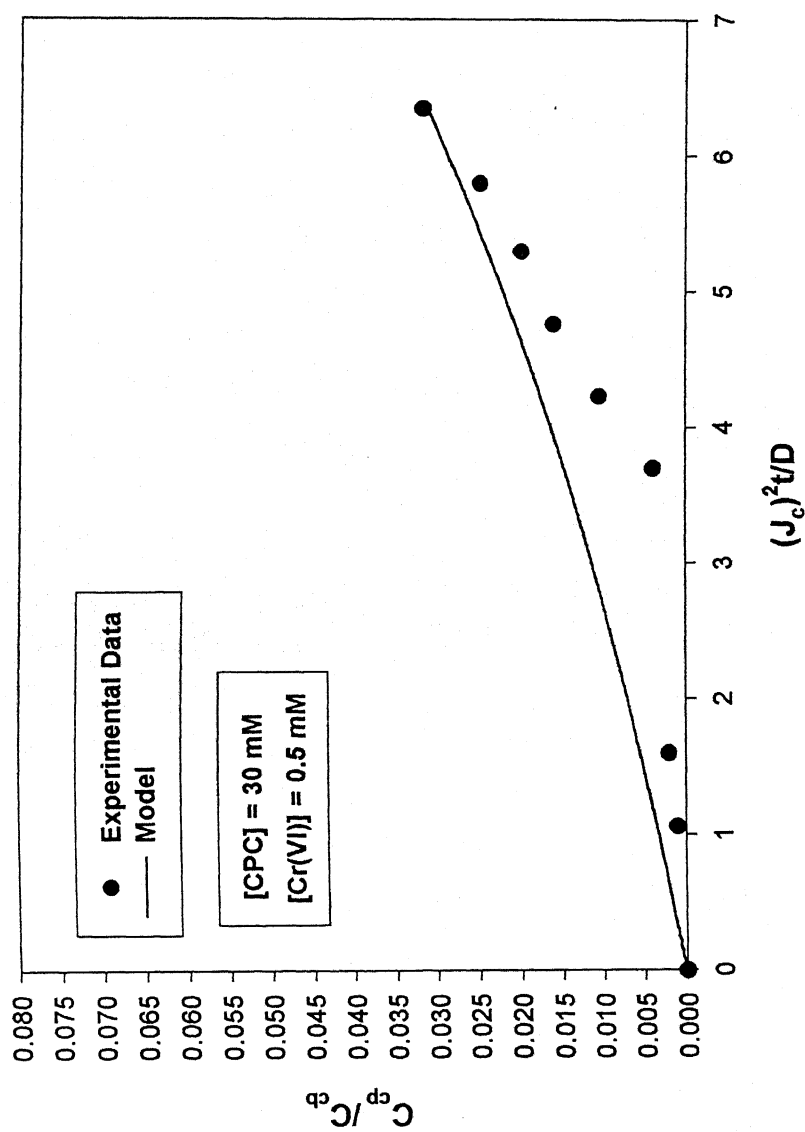


Fig.5.26 Variation of chromate permeate concentration with time

Conclusions and Recommendations

6.1 Conclusions

Micellar Enhanced Ultrafiltration of chromate ions was carried out with 10,000 MWCO membrane using CPC as the surfactant. Based on the experimental studies and the theoretically developed model the following conclusions may be drawn:

1. The permeate flux was found to be constant during an experimental run under constant applied pressure indicating negligible effect of concentration polarization.
2. The increase in pressure leads to increased rejection of CPC. This is due to the compaction of the micellar aggregation layer (MAL).
3. The permeate flux was observed to decline with the increase in feed CPC concentration. The increased resistance offered by MAL to the flow may be the reason behind it.
4. The permeate concentration was found to increase with the feed surfactant concentration under its exclusive runs. Beyond the critical feed concentration (43 mM), the permeate concentration was found to be beyond CMC. This was due to the breaking of micelles into dimmers and trimers.
5. The rejection of chromate in absence of CPC was found to decrease from 10.5 to 3% with the increase in pressure from 376 to 716 kPa. This was attributed due to the fact that the adsorption of chromate on the membrane surface was taking place.
6. With the increase in chromate concentration the permeate flux was found to decrease. The micelles containing metal ions being bigger produce greater resistance to flow.
7. The increase in surfactant concentration leads to an increase in percent retention. However, at very high feed surfactant concentration the percent retention decreased as the chloride ions are preferentially adsorbed on the micelle surface.
8. Pressure was found to have no significant effect on the percent retention. But the permeate flux was found to increase linearly with pressure indicating once more the negligible effect of concentration polarization.
9. Matching between experimental results and predicted values from developed models were found to be close.

6.2 Recommendations

1. The studies may be extended using different MWCO membranes and different surfactants.
2. The effect of temperature on the adsorption of chromate ions on the micelle surface may be investigated.
3. Separate studies may be carried out under stirred condition.
4. Mathematical model has to be improved incorporating the data obtained from semi equilibrium dialysis.

- [1] X. Chai, G. Chen, P. L. Yue and Y. Mi, "Pilot scale membrane separation of electroplating waste water by reverse osmosis", *J. Membrane. Sci.*, **123** (2), 235 - , (1997).
- [2] S.D. Christian, J.F. Scamehorn and R.T. Ellington, in "Surfactant Based Separation Processes"(J.F. Scamehorn and J.H. Harwell, eds.), Markel Dekkar, New York (1989).
- [3] J.H. Markels, S.Lynn and C.J.Radke, "Micellar ultrafiltration in an unstirred batch cell at constant flux", *J. Membrane. Sci.*, **86**, 241-261, (1994).
- [4] J.H. Markels, S.Lynn and C.J.Radke, " Crossflow ultrafiltration of micellar surfactant solutions" , *AIChE.J.* , **41**(a), 2058,(1995).
- [5] K. Kandori and R.S. Schechter, "Selection of surfactants for micellar-enhanced ultrafiltration" , *Sep. Sci. Technol.*, **25**, 83- 108, (1990).
- [6] Z. Sadaoui, C. Azoug, G. Charbit and F. Charbit, " The recovery of hexavalent chromium by micellar enhanced ultrafiltration: influence of operating conditions" , *J. Chem. Eng. Japan*, **30** (5), 799-805, (1997).
- [7] L. Gzara and M. Dhahbi, "Removal of chromate anions by micellar-enhanced ultrafiltration using cationic surfactants", *Desalination*, **137**, 241- 250, (2001).
- [8] D. Gang, S. K. Banerji and T.E. Clevenger, " Chromium removal by modified PVP- coated silica gel", Department of Civil and Environmental Engineering University of Missouri- Columbia.
- [9] V.P. Olivieri (deceased), G.A. Willighan, J.C. Vickers and G. Mc.Gahey, "Continuous microfiltration of secondary waste water effluent", presented at AWWA Membrane Processes.
- [10] E. Korngold, K.Kock and H. Strathmann, "Electrodialysis in advanced waste water treatment", *Desalination*, **24**(1-3), 129-139, (1978).
- [11] J.F. Scamehorn and J.H. Harwell, in "Surfactants in Chemical Process Engineering", (D.T. Wason, M.F. Ginn and D.O. Shah eds), Marcel Dekker, New York (1988).
- [12] J.H.Clint, "Surfactant Aggregation", Chapman and Hall, New York,(1992).

- [13] F. I. Talens-Alession, R. Urbaski and J. Szymanowski, "Evolution of resistance to permeation during micellar enhanced ultrafiltration of phenol and 4- nitrophenol", *Colloids and Surfaces A: Physicochemical and Eng. Aspects*, **178** (1-3), 71-77, (2001)
- [14] H.W. Stache, "Anionic Surfactants", Marcel Dekker, New York (1996).
- [15] R.O. Dunn, Jr., J.F. Scamehorn and S.D. Scamehorn, "Simultaneous removal of dissolved organics and divalent metal cations from water using micellar-enhanced ultrafiltration", *Colloids and Surfaces*, **35** (1), 49-56, (1989).
- [16] S.R. Jaadhav, N. Verma, A. Sharma, P.K. Bhattacharya, "Flux and retention analysis during micellar enhanced ultrafiltration for the removal of phenol and aniline", *Sep. Purification Technology*, **24** (3), 241-250, (2001).
- [17] J. Sabate, M. Pujola, E. Centelles, M. Galan and J. Llorens, "Determination of equilibrium constants of phenol between surfactant micelles and water using ultrafiltering centrifuge tubes", *Colloids and Surfaces A: Physicochemical and Engineering Aspects*, **150** (1-3), 229-245, (1999).
- [18] J.W. Osborne- Lee, R.S. Schechter and W.H. Wade, "Monomer – micellar equilibrium of aqueous solution by the use of ultrafiltration", *J. Colloid Interface Sci.*, **94** (1), 179 (1983).
- [19] J.F. Scamehorn, R.T. Ellington, S.D. Christian, B.W. Penney, R.O. Dunn and N. S. Bhat, "Removal of multivalent metal cations from water using micellar-enhanced ultrafiltration", *AIChE Symposium Series*, **82** (250), 48- 58, (1986).
- [20] A. Shigendo, L. Yang, T. Hiroshi, "Micellar-enhanced ultrafiltration of gold (III) with nonionic surfactants", *J. Membrane Sci.*, **133** (2), 189-194, (1997).
- [21] M. Guardia, E. Peris-Cardells and A. Morales - R. A. Bianco - Prevot and E. Pramauro, "Preconcentration of aluminium by micellar- enhanced ultrafiltration", *Analytica Chimica Acta*, **276** (1), 173- 179, (1993).
- [22] S. Ahmadi, L.K. Tseng, B. Batchelor and S.S. Koseoglu, "Micellar-enhanced ultrafiltration of heavy metals using lecithin", *Sep. Sci. Technol.*, **29** (18), 2435- 2450, (1994).
- [23] S.S. Koseoglu and B. Batchelor, "Removal of toxic heavy metal ions from industrial effluent by MEUF and membrane bioreactors", *Waste Management*, **13**(5-7), (1993).
- [24] B.R. Fillipi, L.W. Brant, J.F. Scamehorn and S.D. Christian, "Use of micellar-enhanced ultrafiltration at low surfactant concentrations and with anionic-nonionic surfactant mixtures", *J. Colloid Interface Sci.*, **213** (1), 68-80, (1999).

- [25] C. Tung, Y. Yang, C. Chang and J. Maa, "Removal of copper ions and dissolved phenol from water using micellar-enhanced ultrafiltration with mixed surfactants", *Waste Management*, In Press.
- [26] Y. Tzeng, H. Tsun and Y. Chang, "Recovery of thuringiensin with cetylpyridinium chloride using micellar-enhanced ultrafiltration process", *Biotechnol. Progress*, **15** (3), 580-586, (1999).
- [27] B. R. Fillipi, J.F. Scamehorn, S.D. Christian, R.W. Taylor, "A comparative economic analysis of copper removal from waste water by ligand modified micellar-enhanced ultrafiltration and by conventional solvent extraction", *J. Membrane Sci.*, **145**, 27-44, (1998).
- [28] E. Jungermann, "Cationic Surfactants", Marcel Dekker, New York.
- [29] M.J. Schick, "Non Ionic Surfactants", Marcel Dekker, New York.
- [30] E.G. Lomax eds., "Amphoteric Surfactants", Marcel Dekker, New York.
- [31] J.H. Clint and T. Walker, "Thermodynamics of micellization of homologous series of n- alkyl methyl sulphoxides and n- alkyl (dimethyl) phosphine oxides", *J. Chem. Soc.*, **71**, 946 (1975).
- [32] M. Cheryan, "Ultrafiltration Handbook", Technomic Publishing, Lancaster, PA (1986).
- [33] M. Syamal, S. De, P.K. Bhattacharya, "Phenol Solubilisation by cetylpyridinium chloride micelles in micellar enhanced ultrafiltration", *J. Membrane Sci.*, **88**, 594 (1982).

Appendix A

A1 Estimation of Hydraulic Membrane Resistance

The hydraulic membrane resistance is given by:

$$R_m = \frac{1}{\mu_w} \left(\frac{\Delta P}{J_w} \right) \quad \text{A1.1}$$

Water permeability of the membrane is given by $\left(\frac{J_w}{\Delta P} \right)$.

Using the data given in Table A1.1, the membrane resistance was found to be $1.85 \times 10^{14} \text{ m}^{-1}$ and the water permeability was 6.59×10^{-12} .

ΔP (kPa)	Water Flux $\times 10^6 \text{ (m/s)}$
376	2.572
580	3.674
716	4.78

Table A1. Water flux vs Applied pressure

A2 Concentration measurement using UV-VIS Spectrophotometer

The permeate concentrations of CPC and hexavalent chromium were calculated from the absorbances of the permeate samples. The absorbances were measured at wavelengths 259nm and 270nm. The molar extinction coefficients of these compounds are listed below.

Wavelength (nm)	Molar extinction coefficient (ϵ)	
	CPC	Cr(VI)
259	3.774	2.884
270	0.895	3.35

Table A2. Molar extinction coefficients

A3 Non –Dimensionalisation of governing equations

To solve the PDE equations *NAG* subroutines was used. Since the non dimensionalised space interval over which *NAG* subroutines can be used range over -1 to 1, the axis of *z* was shifted. Instead of 0 to ∞ , the boundary conditions were estimated at $z = \frac{-D}{2J_w}$ and $z = \frac{D}{2J_w}$.

Transforming time, axial distance, flux and concentration into dimensionless forms by using the characteristic flux (pure water flux, J_w), diffusion coefficient (D) and the characteristic concentration (bulk concentration, C_b) as:

$$\tau = \frac{J_w^2}{D} t ; z^* = \frac{2J_w}{D} z ; J^* = \frac{J(t)}{J_w} \text{ and } C_j^* = \frac{C_j}{C_{b,j}}$$

Therefore, equation 3.28 and 3.30 can respectively be written as:

$$\frac{1}{4} \frac{\partial C_j^*}{\partial \tau} = \frac{\partial^2 C_j^*}{\partial z^{*2}} + \frac{J^*}{2} \frac{\partial C_j^*}{\partial z^*}$$
$$\frac{1}{4} \frac{\partial C_j^*}{\partial \tau} = \left\{ \frac{1}{1 + \frac{K\rho_b}{M}} \right\} \left[\frac{\partial^2 C_j^*}{\partial z^{*2}} + \frac{J^*}{2} \frac{\partial C_j^*}{\partial z^*} \right]$$

The initial and boundary conditions can be modified as follows:

$$\text{at } \tau = 0, C_j^* = 1.0$$

$$\text{at } z^* = -1, C_j^* = 1.0$$

$$\text{at } z^* = 1, J^* C_m^* R_r = \frac{\partial C_m^*}{\partial z^*}$$

Appendix B

Experimental Data of MEUF Experiments

Time(min)	Percent Rejection		
	[CPC] = 0.1mM	[CPC] = 0.1mM	[CPC] = 0.1mM
10	78.5429	78.6000	85.8900
20	71.9890	75.1600	83.2000
30	64.4500	69.4190	77.3750
40	55.9800	64.2020	73.4500
50	51.0300	60.7400	69.3920
60	35.7500	55.7720	65.2940
70		52.9760	62.9750
80	36.7170	50.5130	62.1624
90		49.7100	61.1750
100	34.2470	48.8600	60.9330
110		49.8700	58.9770
120	29.7890	50.4060	58.8900

Table B1 Percent Rejection vs. time for CPC below CMC

Time(min)	Permeate Flux *10 ⁶ (m/s)			Percent Rejection		
	$\Delta P = 376kPa$	$\Delta P = 580kPa$	$\Delta P = 716kPa$	$\Delta P = 376kPa$	$\Delta P = 580kPa$	$\Delta P = 716kPa$
10	1.6210	2.5900	3.3500		99.398	99.357
20	1.6210	2.5800	3.3000	98.790	99.112	99.215
30	1.6210	2.5720	3.3000	98.80	98.860	98.961
40	1.6210	2.5720	3.3000	98.60	98.607	98.814
50	1.6200	2.5720	3.3000	98.301	98.392	98.725
60	1.6200	2.5720	3.3000	98.250	98.372	98.67
70	1.6200	2.5720	3.3000	98.140	98.246	98.56
80	1.6210	2.5720	3.3000	98.1325	98.179	98.502
90	1.6200	2.5720	3.3000	97.90	98.108	98.425
100	1.6200	2.5720	3.3000	97.80	97.90	98.438
110	1.6200	2.5720	3.3000	97.80	97.956	98.316
120	1.6200	2.5720	3.3000	97.75	97.90	98.355

Table B2 Permeate Flux and CPC Rejection vs. time at feed CPC = 30 mM

Feed CPC conc.(mM)	Unstirred Cell		Stirred Cell	
	Permeate Flux *10 ⁶ (m/s)	Permeate CPC conc.(mM)	Permeate Flux *10 ⁶ (m/s)	Permeate CPC conc.(mM)
0.1	5.140	0.0780	5.987	0.0787
0.3	3.674	0.142	4.335	0.1599
0.5	3.538	0.196	4.041	0.1915
10.0	2.7599	0.2059		
30.0	2.5720	0.5677		
40.0	2.530	0.877		
60.0	1.870	1.36		

Table B3 Permeate Flux and Permeate Concentration of CPC in stirred and unstirred cell

Time(min)	Permeate Flux *10 ⁶ (m/s)			Percent Rejection		
	$\Delta P = 376kPa$	$\Delta P = 580kPa$	$\Delta P = 716kPa$	$\Delta P = 376kPa$	$\Delta P = 580kPa$	$\Delta P = 716kPa$
10	3.6700	5.5100	5.8780	53.1500	26.7040	28.7400
20	3.6700	5.1400	5.8780	26.0430	7.4200	7.1960
30	3.5300	4.9970	5.7870	7.6060	5.0530	3.9450
40	3.5300	4.9970	5.7570	4.8007	4.5800	3.5300
50	3.5300	4.9970	5.5100	3.6800		2.5990
60	3.5300	4.9970	5.5100	3.5470	1.6123	2.5290
70	3.5300	4.9970		3.4930	2.8920	2.2760
80	3.5300	4.9970	5.5100	3.5890	4.2180	2.1840
90	3.5300	4.9970	5.5100	3.2630	2.9306	1.8220
100	3.5300	4.9970		2.9480	2.9306	1.8400
110	3.5300	4.9970	5.5100	10.7300	3.8010	2.3100

Table B4 Permeate Flux and Permeate Concentration of Cr(VI) vs. time

Feed CPC concentration 30 mM					
	Permeate Flux*10 ⁶ (m/s)				
Time (min)	0.3 mM	0.5 mM	0.7 mM	1.0 mM	1.5 mM
10	2.720	2.471	2.204	2.160	1.896
20	2.720	2.415	2.204	2.160	1.896
30	2.720	2.415	2.200	2.150	1.896
40	2.710	2.415	2.200	2.150	1.896
50	2.710	2.413	2.200	2.150	1.896
60	2.710	2.413	2.180	2.150	1.895
70	2.700	2.413	2.180	2.140	1.894
80	2.700	2.410	2.180	2.140	1.893
90	2.700	2.410	2.180	2.140	1.892
100	2.700	2.410	2.180	2.140	1.892
110	2.690	2.410	2.170	2.140	1.892
120	2.690	2.410	2.170	2.140	1.892

Table B5 Permeate Flux vs. time at feed CPC = 30 mM

Feed CPC concentration 30 mM					
	Percent Rejection				
Time (min)	0.3 mM	0.5 mM	0.7 mM	1.0 mM	1.5 mM
10		97.620	96.857	97.190	97.522
20	99.990	99.990	99.447	99.370	98.490
30	99.980		99.975	99.990	98.900
40	99.970	99.990	99.658	99.700	98.840
50	99.950	99.950	99.657	99.403	99.070
60	99.317	99.920	99.184	98.574	98.825
70	98.937	99.900	99.078	98.495	98.782
80	96.500	99.610	98.535	98.110	98.500
90	95.477	98.393	98.247	97.190	97.870
100	98.130	98.856	96.570	99.370	98.345
110		97.620	96.857	99.990	97.522
120		99.990	99.447		98.490

Table B6 Percent Rejection vs. time at feed CPC = 30 mM

Feed Chromate concentration 0.3 mM					
	Permeate Flux*10 ⁶ (m/s)				
Time (min)	1.0 mM	5.0 mM	10.0 mM	30.0 mM	60.0 mM
10	2.810	2.750	2.720	2.572	1.870
20	2.820	2.750	2.720	2.572	1.880
30	2.810	2.750	2.720	2.572	1.870
40	2.800	2.730	2.710	2.572	1.880
50	2.800	2.750	2.710	2.570	1.870
60	2.810	2.750	2.710	2.570	1.870
70	2.810	2.730	2.710	2.570	1.880
80	2.800	2.720	2.700	2.570	1.890
90	2.820	2.750	2.710	2.568	1.870
100	2.800	2.730	2.700	2.568	1.870
110	2.810	2.750	2.700	2.570	1.870
120	2.810	2.750	2.710	2.568	1.870

Table B7 Permeate Flux vs. time at feed Chromate = 0.3 mM

Feed Chromate concentration 0.3 mM					
	Percent Rejection				
Time (min)	1.0 mM	5.0 mM	10.0 mM	30.0 mM	60.0 mM
10	67.660	85.200	96.567	98.800	99.500
20	69.860	92.800	98.767	99.400	99.300
30	71.640	93.560	99.784	99.530	99.400
40	73.503	92.860	99.983	99.600	99.200
50	73.563	92.250		99.535	99.120
60	73.625	92.650	99.815	99.317	96.820
70	73.984		99.618	98.937	95.260
80	75.539	92.900	98.768	96.500	94.500
90	75.960	92.580	98.160	95.477	
100	76.692	92.080		98.130	94.100
110	76.380	93.350	97.737	95.670	92.860
120	76.323	92.400	95.437	96.330	91.600

Table B8 Percent Rejection vs. time at feed Chromate = 0.3 mM

Permeate Flux*10 ⁶ (m/s)					
CPC conc. (mM)	0.3 mM	0.5 mM	0.7 mM	1.0 mM	1.5 mM
1	2.81			1.44	
5	2.80	2.72	1.898	1.622	
10	2.72	2.572	2.204	2.013	1.906
30	2.57	2.417	2.204	2.160	1.896
60	1.87			1.839	1.800

Table B9 Permeate Flux vs. time

Percent Rejection					
CPC conc. (mM)	0.3 mM	0.5 mM	0.7 mM	1.0 mM	1.5 mM
1	76.43			42.51	
5	93.65	91.96	92.38	88.64	
10	99.20	99.53	97.60	96.56	95.80
30	99.53	99.83	99.04	98.84	98.78
60	96.9				75.02

Table B10 Percent Rejection vs. time

Feed CPC concentration 30 mM		
	Permeate Flux*10 ⁶ (m/s)	Percent Rejection of Cr(VI)
$\Delta P = 376kPa$	1.409	99.83
$\Delta P = 580kPa$	2.5	99.828
$\Delta P = 716kPa$	3.425	99.826

Table B11 Permeate Flux and Percent Rejection vs. Pressure at [Cr(VI)] = 0.5mM

Appendix C

Adsorption equilibrium constants calculated with MEUF Data

CPC conc. (mM)	K_{ad} (ml/g)
5	177.42
10	237.137
30	11830.4
60	1671.52

Table C1 Variation of K_{ad} with surfactant concentration

Appendix D

SED Experimental Data

Feed CPC conc. = 30 mM				Feed CPC conc. = 10 mM		
Concentration of Chromate (mM) in Permeate Compartment						
Time(hr)	0.5 mM	0.7 mM	1.0 mM	0.5 mM	0.7 mM	1.0 mM
4	0.00177	0.01234	0.0023	0.00059	0.013	
8	0.00522	0.00580	0.0724	0.00442		0.005186
16	0.00398	0.00237		0.00620	0.017	0.006102
22	0.00172	0.00637	0.0362	0.00425	0.018	0.007256
24	0.00169	0.00627	0.0349	0.00587	0.020	0.007176

Table D1 Chromate conc. in permeate compartment vs. time

Adsorption isotherm of chromate using the SED data is shown in the plot.

Appendix E

Physical Property	Value
Diffusivity of CPC	$1.8 \times 10^{-10} \text{ (m}^2/\text{s)}$
Critical micelle conc. of CPC in 0.01M NaCl	$8.8 \times 10^{-4} \text{ M} = 0.3 \text{ kg/m}^3$
Aggregation number of CPC	136 monomers/micelle
Monomer hydrodynamic radius	0.42 nm
Micelle hydrodynamic radius	2.5 nm

Table E1 Physical constants of surfactant

Appendix F

Sample Calculation

$$\lambda_1 = 259 \text{ nm}$$

1 = cetyl pyridium chloride

$$\lambda_2 = 270 \text{ nm}$$

2 = hexavalent chromium

Since the cell thickness is always constant, using Beer's Law $A_\lambda = a_\lambda LC$

$$a_{1, \lambda_1} = 3.774$$

$$a_{2, \lambda_1} = 2.884$$

$$a_{1, \lambda_2} = 0.895$$

$$a_{2, \lambda_2} = 3.35$$

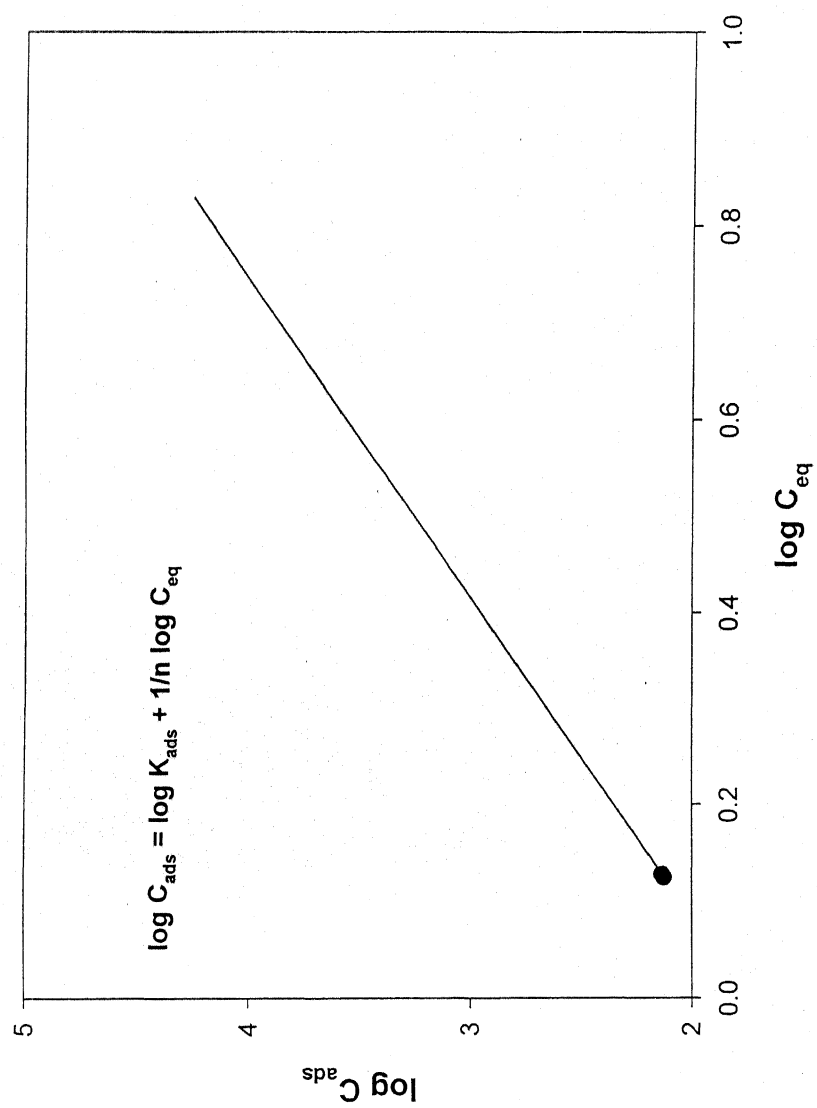
A_{λ_1} = solution absorbance at λ_1

A_{λ_2} = solution absorbance at λ_2

Considering $A_{\lambda_1} = 1.357$ and $A_{\lambda_2} = 0.327$, we get,

$$C_1 = \frac{3.35 \times 1.357 - 2.884 \times 0.327}{3.774 \times 3.35 - 0.895 \times 2.884} = 0.358 \text{ mM}$$

$$C_2 = \frac{3.774 \times 0.327 - 0.895 \times 1.357}{3.774 \times 3.35 - 0.895 \times 2.884} = 1.946 \times 10^{-3} \text{ mM}$$



Freundlich plot for adsorption of Cr(VI) on the micelle surface using SED data